JOURNAL OF QUATERNARY SCIENCE (2023) **38**(7) 1044–1061 ISSN 0267-8179. DOI: 10.1002/jqs.3525

JQS Journal of Quaternary Science QRA Quaternary Research Association

Climatic control on the retreat of the Laurentide Ice Sheet margin in easternmost Québec–Labrador (Canada) revealed by cosmogenic nuclide exposure dating

PIERRE-OLIVIER COUETTE,[1,2]* JEAN-FRANÇOIS GHIENNE,[2] PATRICK LAJEUNESSE[1] and JÉRÔME VAN DER WOERD[2]
[1]Département de Géographie, Université Laval, Québec, Canada
[2]Institut Terre & Environnement de Strasbourg (ITES), UMR 7063, CNRS, Université de Strasbourg, Strasbourg, France

Received 28 October 2022; Revised 27 March 2023; Accepted 10 April 2023

ABSTRACT: The Laurentide Ice Sheet (LIS) was the largest ice sheet in the Northern Hemisphere during the last glacial cycle. The effects of its demise on global climate and sea-level changes during the subsequent deglaciation are unequivocal. Understanding the interplay between ice sheets and long-term or short-term (e.g. abrupt) climatic events is therefore crucial for predicting future rates of ice sheet melting and their potential contribution to sea-level changes. Here, we present 37 new ^{10}Be surface exposure ages from easternmost Québec–Labrador that allow us to identify close ties between regional deglaciation history and climate. These results reveal that the LIS was disconnected from the Newfoundland Ice Cap by ~14.1 ka. Samples collected from moraine boulders indicate that this event was followed by five major stillstands and/or readvance stages of the LIS margin. Integrating our new moraine ages with those of earlier studies allows us to depict a temporal framework including events at ~12.9, ~11.5, ~10.4, ~9.3 and ~8.4–8.2 ka. These moraine ages highlight a strong sensitivity of the LIS to temperature changes in the Northern Hemisphere, as the documented continental ice margin stabilizations coincide with abrupt cooling events recorded in Greenland ice cores. These observations support the idea of a negative feedback mechanism induced by meltwater forcings into the North Atlantic Ocean which, in turn, provoked repeated cold reversals during the Younger Dryas and early Holocene. © 2023 John Wiley & Sons, Ltd.

KEYWORDS: abrupt climatic events; cosmogenic ^{10}Be exposure dating; deglaciation; Laurentide Ice Sheet; moraines; Québec–Labrador

Introduction

The ice sheets that once covered the Northern Hemisphere played an undeniable role in modulating global changes since the Last Glacial Maximum (LGM), as their growth and decay were closely interconnected with atmospheric/oceanic circulation and sea-level changes (Alley et al., 1997; Clark et al., 2000; Carlson et al., 2008; Denton et al., 2010; Briner et al., 2020; Lowell et al., 2021). Warming conditions during the deglaciation that followed the LGM provoked enhanced freshwater inputs into the North Atlantic Ocean, slowing the Atlantic Meridional Overturning Circulation (AMOC) and ultimately reducing air temperature over the Northern Hemisphere (Barber et al., 1999; Fisher et al., 2002; McManus et al., 2004; Rohling & Pälike, 2005; Carlson & Clark, 2012; Jennings et al., 2015; Süfke et al., 2022). However, the interplay between such feedbacks and ice mass evolution is still poorly constrained, as Holocene climate evolution and its sensitivity to known forcings remain in some cases elusive (Axford et al., 2009; Jennings et al., 2015; He & Clark, 2022). Documenting the response of former ice sheets –such as the Laurentide Ice Sheet (LIS)– to external forcing, and the timing of this response, is critical for assessing the contribution of melting ice masses to past and future sea-level rise.

The study of stillstands and readvances of the LIS margin during its overall retreat provide key information on late Wisconsinan and early Holocene climate fluctuations, which is essential for (i) improving our knowledge on the long-term glacial and deglaciation history of former ice sheets, (ii) determining their sensitivity to climate change and (iii) identifying trigger mechanisms of ice margin behaviour (Lesnek & Briner, 2018; Briner et al., 2020; Young et al., 2020). Identification of causes, such as drainage of large glacial lakes, contributes to assessing their potential role in, and response to, millennial-scale abrupt climatic events (e.g. Fisher et al., 2002; Lajeunesse & St-Onge, 2008; Yu et al., 2010; Dubé-Loubert et al., 2018; Leydet et al., 2018; Brouard et al., 2021; Süfke et al., 2022). Dating and reconstructing the evolution of former ice sheet margins is therefore crucial for understanding the long-term interconnections between ice sheets and the global climate system and identifying the interfering feedback mechanisms that influence deglaciation (Briner et al., 2020; Lowell et al., 2021).

The development of cosmogenic exposure dating has contributed substantially to improving reconstructions of the deglacial history in North America by allowing direct dating of landforms deposited during stagnation or retreat stages of ice margins (Balco, 2020). Over the last few decades, an ever growing number of studies have focused on identifying and dating major stillstands and readvances of the LIS margin during its retreat following the LGM (i.e. Marsella et al., 2000; Clark et al., 2003; Briner et al., 2005, 2007, 2009; Balco et al., 2009; Young et al., 2012, 2020a, 2021; Bromley

*Correspondence: Pierre-Olivier Couette, as above.
Email: pierre-olivier.couette.1@ulaval.ca

et al., 2015; Davis et al., 2015; Ullman et al., 2016; Margreth et al., 2017; Crump et al., 2020; Lowell et al., 2021). However, as these studies focused mostly on specific sectors of the LIS, large geographical gaps in available absolute ages from glacial landforms remain, especially at its eastern fringe. Despite the relatively large number of radiocarbon ages available in southern Labrador and adjacent easternmost Québec that provide minimum-limiting ages for deglaciation (i.e. King, 1985; Dyke et al., 2003; Dalton et al., 2020), the chronology of most of the major moraine systems marking stabilizations/readvances of the retreating LIS margin in the region is still poorly constrained.

In this paper, we report on the deglaciation history of the eastern sector of the LIS by using terrestrial cosmogenic ^{10}Be exposure dating of boulders from major moraine systems. This chronological dataset coupled with previously published and new radiocarbon ages allow us to (1) constrain the position of the ice margin during its retreat, and (2) assess retreat rates of the ice margin in order to identify time intervals of important changes. These results provide a revised deglacial chronological framework across five former ice-marginal stillstand/readvance positions located along a 500-km-long transect from the coast to the Labrador hinterland. These results allow us to discuss the potential causes for deposition of moraines in easternmost Québec–Labrador and their implications for regional climate.

Regional setting

Easternmost Québec–Labrador (Canada) hosts a series of moraines marking the overall retreat of the LIS during the Lateglacial and early Holocene (Fig. 1). The region lies within the Grenville geological province of the Canadian Shield and is underlain mainly by Proterozoic quartzofeldspathic gneisses, granites and anorthosites (Greene, 1974; Hynes & Rivers, 2010). Regional physiography consists of a hilly 'peneplain' ranging from 300 to 500 m in elevation that is deeply incised by structural valleys. The study area also includes the Lake Melville depression, an estuary that stretches 200 km inland from the Atlantic coast, and the Mealy Mountain Massif, a prominent plateau-topped highland reaching over 1000 m. Except for the area located to the northwest of Lake Melville, the study area is characterized by a generally thin ice-contact cover of deposits and valleys partially filled with glaciomarine to glaciofluvial deposits (Fulton & Hodgson, 1979; King, 1985). Five extensive morainic systems (>100 km long) previously identified in easternmost Québec–Labrador represent major successive positions of the retreating LIS margin following the late Wisconsinan glacial cycle (i.e. from SE to NW: Brador, Belles Amours, Paradise, Little Drunken and Sebaskachu moraine systems: Fulton & Hodgson, 1979; King, 1985; Occhietti et al., 2011). Although these moraines undeniably represent mappable, regional-scale stillstands and/or potential readvances of the LIS margin, their age remains poorly constrained and their correlations with other sectors of the LIS to the north (e.g. Baffin Island) or to the west (e.g. St. Lawrence estuary) are still debated (e.g. King, 1985; Grant, 1992; Occhietti et al., 2011).

Early workers proposed that easternmost Québec–Labrador was not covered by the LIS during the late Wisconsinan glaciation (Coleman, 1921). The idea of a restricted LIS in the region was later invoked: some authors positioned the LGM margin of the LIS at the Brador Moraine near the present coastline (Ives, 1978; Vilks & Mudie, 1978) and others suggested that it was located even more inland at the Paradise Moraine based on the scarcity of geomorphological evidence further east (Fig. 1; Fulton & Hodgson, 1979). In more recent investigations, severals authors revised this restricted position by demonstrating that the LIS completely covered easternmost Québec-Labrador at the LGM, reaching as far as the shelf edge in the Labrador Sea (Josenhans et al., 1986; Piper, 1991; Grant, 1992; Roger et al., 2013). After its separation from the Newfoundland Ice Cap, the LIS margin stabilized at a position located at the modern coast of eastern Québec–Labrador, depositing the Brador and the Belles Amours moraine systems (Fig. 1; Grant, 1992). The age of the Brador and the Belles Amours moraine systems were estimated at 12.5 ^{14}C ka BP (~15 cal ka BP) and 11.0 ^{14}C ka BP (~13 cal ka BP), respectively (King, 1985). Grant (1992) proposed that the LIS margin stabilized when it grounded at the marine limit to build the Brador Moraine at 12.6 ^{14}C ka BP (~15 cal ka BP) and deposited the Belles Amours Moraine shortly after (<200 years) in the frame of a regional readvance. The ice margin then retreated westward and deposited successively the Paradise and Little Drunken moraine systems during two stillstands and/or readvances of the LIS margin (King, 1985). The Paradise Moraine was proposed to correspond to the Younger Dryas (YD) event, therefore correlating to the St-Narcisse Moraine of southern Québec (Dyke & Prest, 1987; King, 1985; Grant, 1992; Occhietti, 2007), while the Little Drunken Moraine was speculated to correspond to the Québec North Shore Moraine deposited at ~10.8 cal ka BP (Dubois & Dionne, 1985; Dietrich et al., 2019). However, the abandonment of the Paradise Moraine and Québec North Shore Moraine have been recently dated at 10.3 ± 0.6 and 9.2 ± 0.5 ka, respectively, using cosmogenic exposure dating (Ullman et al., 2016). After this stage of deglaciation, the LIS margin stabilized again at the west end of Lake Melville and deposited the Sebaskachu Moraine. The Little Drunken Moraine has been tentatively correlated to the Sebaskachu Moraine by several authors (i.e. Blake, 1956; Fulton & Hodgson, 1979; Occhietti et al., 2011), although no formal geomorphological connection has been observed between the two systems. The ice margin is estimated to have retreated from the Sebaskachu Moraine position at 8.0 ^{14}C ka BP (~8.8 cal ka BP) and reached central Labrador by 7.0 ^{14}C ka BP (~7.8 cal ka BP; King, 1985). Similarly, cosmogenic exposure dating on erratic boulders yielded ages of 8.6 ± 0.6 ka west of Lake Melville and 7.5 ± 0.4 ka for central Labrador (Ullman et al., 2016). Ice retreat then took place rapidly with the final ablation of the LIS at ~5.5 ^{14}C ka BP (~6.0 cal ka BP) over the central Québec–Labrador Peninsula (Richard et al., 1982; Clark et al., 2000; Jansson, 2003; Occhietti et al., 2011; Dubé-Loubert et al., 2018), leaving series of small recessional moraines across the landscape.

Methods

Field mapping and sampling

Positions of the former margins (i.e. moraines) of the LIS were mapped to spatially constrain its successive extents during deglaciation of the easternmost Québec–Labrador sector (Fig. 1). Our mapping builds upon previous investigations on moraines across the study area that was, however, sporadic and not sufficiently constrained in some sectors (Dubois & Dionne, 1985; Grant, 1992; Klassen et al., 1992). Interpretation of Landsat satellite imagery allowed us to refine and extend previous maps of moraine deposits. All mapped moraine systems were then visited in the field and sampled. Additionally, the chronology (^{10}Be and ^{14}C) was used to interpolate ice margin positions in areas lacking well-preserved moraine deposits.

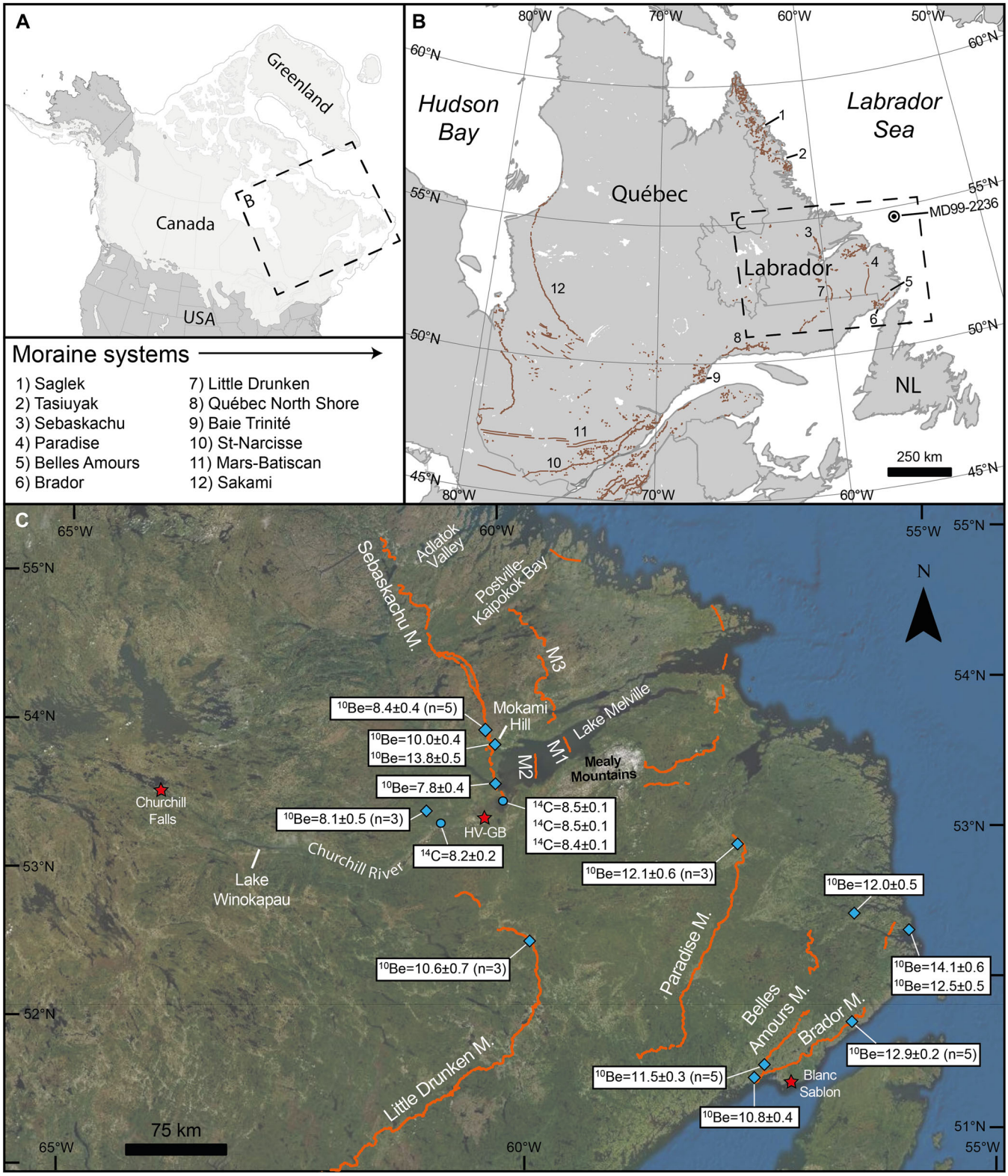

Figure 1. Location of the study area with mapped moraine systems. (A) Extent of the ice cover (light grey) in North America during the Last Glacial Maximum, modified from Dalton et al. (2020). (B) Location of mapped moraine systems of the LIS discussed in this study, modified from Occhietti et al. (2011). NL: Newfoundland. (C) Easternmost Québec–Labrador and major moraine systems presented in this study. Sample locations of our new cosmogenic ^{10}Be ages are represented by diamonds and radiocarbon ^{14}C ages are represented by circles. All ages are reported in thousand years (ka). M1, M2, M3: unnammed moraine systems within and north of Lake Melville, respectively, from Syvitski and Lee (1997), Gebhardt et al. (2020) and Batterson et al. (1987). Red stars represent localites mentionned in the text. HV-GB: Happy Valley–Goose Bay. [Color figure can be viewed at wileyonlinelibrary.com]

Surface exposure ages on moraine boulders, erratics and bedrock outcrops were obtained using cosmogenic beryllium-10 dating (hereafter referred to as ^{10}Be; Fig. 2). About 1 kg of rock was collected from the upper 2 cm of boulder surfaces using a handheld rocksaw, a hammer and a chisel. The flat top of stable boulders embedded in the moraine matrix was targeted to minimize overturning possibility, post-deposition exhumation and extreme weathering. Where available, quartz veins or quartz-rich material were extracted from the boulders. Samples were precisely documented in the field, including site description, coordinates and elevation obtained from a handheld GPS.

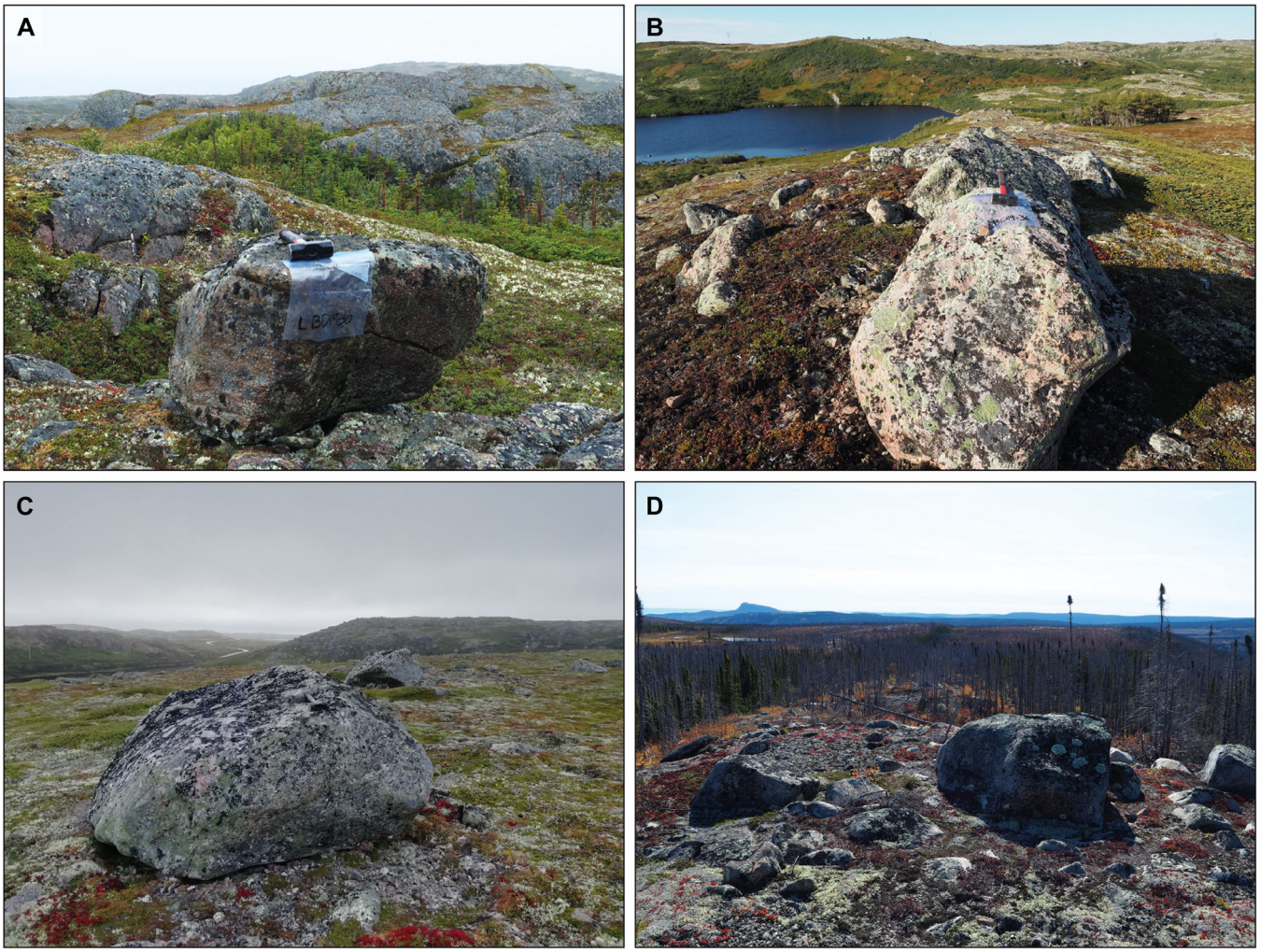

Figure 2. Examples of representative samples collected in easternmost Québec–Labrador. (A) Sample LBD19-30 from a coastal erratic (14.1 ± 0.6 ka). (B) Sample LBD19-36 from the Belles Amours Moraine (11.8 ± 0.4 ka). (C) Sample LBD19-43 from the Brador Moraine (12.8 ± 0.5 ka). (D) LBD19-68 from the Sebaskachu Moraine (8.2 ± 0.4 ka). [Color figure can be viewed at wileyonlinelibrary.com]

Sample preparation and analysis

Samples were processed at the cosmogenic nuclide laboratory at the University of Strasbourg following a well-established protocol modified from Kohl and Nishiizumi (1992) and Bierman et al. (2002). All samples were crushed and sieved to isolate the 250–1000 μm fraction, which was subsequently treated by leaching in an HCl solution to eliminate oxides and organic material. Up to nine ultrasonic leaching cycles with diluted HF and HNO_3 (~1% each) solution were needed to purify the quartz. A commercial ^{9}Be carrier (~0.25–0.5 mg) was added to the samples before dissolving the pure quartz in concentrated HF (48%) and HNO_3 (68%). Beryllium was isolated through anion and cation exchange columns and then precipitated as hydroxide. Beryllium hydroxide was dried and calcinated to BeO at 750°C. ^{10}Be/^{9}Be ratios were measured at ASTER, the French Accelerator Mass Spectrometry (AMS) at CEREGE (Aix-en-Provence). The measurements of samples were normalized against an in-house CEREGE standard, STD11, with an assumed ^{10}Be/^{9}Be ratio of $(1.191 \pm 0.013) \times 10^{-11}$ (Braucher et al., 2015) and a ^{10}Be half-life of 1.387 ± 0.012 Ma (Chmeleff et al., 2010; Korschinek et al., 2010). A procedural blank was processed with each batch of samples to evaluate ^{10}Be contamination during laboratory procedures. Blank ^{10}Be/^{9}Be ratios range from $5.21 \pm 0.42 \times 10^{-15}$ to $6.12 \pm 0.45 \times 10^{-15}$; average blank ^{10}Be/^{9}Be ratios were $5.74 \pm 0.59 \times 10^{-15}$ ($n = 8$) (Table 1).

^{10}Be age calculations

^{10}Be ages were calculated using the online exposure age calculator formerly known as the CRONUS-Earth online exposure age calculator version 3.0 (Balco et al., 2008; https://hess.ess.washington.edu/). Calibration was done using the northeastern North America (NENA) ^{10}Be production rate of 4.04 ± 0.27 atoms g^{-1} a^{-1} (Balco et al., 2009) and the nuclide- and time-dependent LSDn scaling scheme (Lifton et al., 2014). The NENA production rate is statistically identical to other high-latitude production-rate calibration datasets such as the Baffin Bay (Young et al., 2013) and the Rannoch Moor (Putnam et al., 2019) production rates. For comparison, the global production rate (Borchers et al., 2016) would result in ages that are ~5% younger. By comparison, using the St or Lm scaling schemes (Lal, 1991; Stone, 2000) would result in exposure ages that are ~5% older than the LSDn-derived ^{10}Be ages. The effects of postglacial erosion on ^{10}Be ages were neglected as sampled bedrock and boulder surfaces commonly displayed glacial striations, suggesting little surface erosion since deglaciation. Topographic shielding was not taken into account for boulders and sampled surfaces as it was estimated to be negligible (<1%). Glacio-isostatic uplift corrections were not accounted for in the final results (Supporting Information Table S1), as its effects on cosmogenic nuclide production are not well constrained (Balco et al., 2009; Young et al., 2020b). Snow cover corrections were also omitted in the calculation of the ages as we sampled boulders

Table 1. Sample characteristics, AMS measurement results and ^{10}Be ages.

Sample no.	Latitude (DD)	Longitude (DD)	Altitude (m)	Quartz (g)	Carrier (mg)	^{10}Be/^{9}Be (10^{-14})	Blank ^{10}Be/^{9}Be (10^{-14})	^{10}Be concentration (atoms g^{-1})	^{10}Be age (a)
Brador Moraine									**12 930 ± 240 (700)**
LBD19-32	51.7933	−56.3825	162	6.7401	0.26480	3.08 ± 0.17	0.60 ± 0.09	64 896 ± 3581	12 613 ± 698
LBD19-33	51.7942	−56.3800	152	39.7256	0.48679	8.56 ± 0.27	0.59 ± 0.06	65 264 ± 2062	12 814 ± 406
LBD19-40	51.4997	−57.3684	138	9.6414	0.26606	4.09 ± 0.18	0.60 ± 0.09	64 380 ± 2853	12 873 ± 572
LBD19-42	51.4985	−57.3560	147	22.8433	0.51638	5.05 ± 0.17	0.61 ± 0.04	67 092 ± 2662	13 367 ± 557
LBD19-43	51.5075	−57.3217	142	28.7180	0.48375	6.37 ± 0.22	0.60 ± 0.07	64 999 ± 2269	12 945 ± 453
Belles Amours Moraine									**11 500 ± 340 (670)**
LBD19-34	51.5021	−57.3821	167	13.9409	0.26473	5.14 ± 0.21	0.60 ± 0.09	57 631 ± 2371	11 163 ± 461
LBD19-35	51.5031	−57.3813	170	11.5690	0.26497	4.58 ± 0.20	0.60 ± 0.09	60 894 ± 2636	11 785 ± 512
LBD19-36	51.5044	−57.3812	168	28.1845	0.51652	5.64 ± 0.18	0.60 ± 0.07	61 733 ± 6404	11 972 ± 383
LBD19-38	51.5040	−57.3928	168	30.0281	0.51833	5.60 ± 0.21	0.60 ± 0.07	57 695 ± 2181	11 163 ± 423
LBD19-39	51.5044	−57.3926	168	17.8025	0.26348	6.46 ± 0.30	0.55 ± 0.06	58 502 ± 2730	11 334 ± 530
Paradise Moraine									**12 140 ± 560 (890)**
LBD19-53	53.0460	−57.4695	193	30.0222	0.51350	10.37 ± 0.33	0.60 ± 0.07	111 734 ± 3518	20 805 ± 658*
LBD19-54	53.0458	−57.4691	195	30.0476	0.51406	18.06 ± 0.57	0.60 ± 0.07	199 659 ± 6300	37 116 ± 1182*
LBD19-56	53.0453	−57.4659	201	30.0862	0.51683	5.98 ± 0.22	0.60 ± 0.07	61 830 ± 2303	11 420 ± 427
LBD19-57	53.0449	−57.4638	199	16.2079	0.26464	6.64 ± 0.26	0.55 ± 0.06	66 552 ± 2573	12 328 ± 478
LBD19-58	53.0468	−57.4650	196	28.6727	0.50936	6.37 ± 0.22	0.60 ± 0.07	68 549 ± 2484	12 747 ± 463
Little Drunken Moraine									**10 640 ± 670 (960)**
LBD19-63	52.4698	−59.8250	483	40.0595	0.52240	12.40 ± 0.42	0.59 ± 0.06	102 959 ± 3451	14 749 ± 496*
LBD19-64	52.4699	−59.8256	492	40.1026	0.52521	11.44 ± 0.37	0.59 ± 0.06	94 976 ± 3030	13 483 ± 432*
LBD19-65	52.4680	−59.8236	491	3.1706	0.21502	2.29 ± 0.12	0.53 ± 0.06	79 756 ± 4431	11 291 ± 629
LBD19-66	52.4678	−59.8234	490	40.0764	0.51965	8.58 ± 0.31	0.59 ± 0.06	69 260 ± 2469	9803 ± 350
LBD19-67	52.4696	−59.8258	493	40.0306	0.51763	9.70 ± 0.30	0.59 ± 0.06	78 693 ± 2475	11 112 ± 350
Sebaskachu Moraine									**8350 ± 420 (630)**
LBD19-68	53.9088	−60.2298	351	25.6098	0.51636	4.40 ± 0.18	0.55 ± 0.06	51 821 ± 2069	8204 ± 328
LBD19-69	53.9092	−60.2296	348	27.0470	0.51460	4.46 ± 0.18	0.55 ± 0.06	49 764 ± 2021	7914 ± 322
LBD19-70	53.9091	−60.2296	348	25.4056	0.51304	4.76 ± 0.18	0.55 ± 0.06	56 886 ± 2117	9082 ± 339
LBD19-71	53.9096	−60.2296	347	40.0772	0.52268	6.74 ± 0.23	0.59 ± 0.06	53 605 ± 1847	8534 ± 295
LBD19-73	53.9108	−60.2297	347	26.7774	0.51674	4.43 ± 0.20	0.55 ± 0.06	50 109 ± 2214	7973 ± 353
Peter's Moraine									**8090 ± 460 (680)**
LBD19-16	53.3786	−60.9337	172	21.9378	0.51781	3.35 ± 0.14	0.59 ± 0.05	43 577 ± 2012	8250 ± 382
LBD19-17	53.3788	−60.9341	170	22.3020	0.51957	3.52 ± 0.14	0.61 ± 0.04	45 240 ± 2040	8598 ± 389
LBD19-18	53.3770	−60.9374	163	30.9066	0.51881	2.75 ± 0.11	0.61 ± 0.04	35 473 ± 1629	6827 ± 314*
LBD19-19	53.3769	−60.9369	163	40.1043	0.51455	8.07 ± 0.28	0.59 ± 0.05	64 171 ± 2544	12 363 ± 492*
LBD19-20	53.3785	−60.9322	163	20.6205	0.52079	2.92 ± 0.12	0.61 ± 0.04	39 074 ± 1760	7500 ± 338
LBD19-28	52.5126	−56.2455	141	37.7807	0.51529	7.30 ± 0.23	0.59 ± 0.05	61 183 ± 2293	12 024 ± 452
LBD19-30	52.3696	−55.6632	140	35.0651	0.51566	7.86 ± 0.28	0.59 ± 0.05	71 479 ± 2950	14 104 ± 584
LBD19-31	52.3689	−55.6641	137	40.0454	0.51928	7.92 ± 0.26	0.59 ± 0.05	63 520 ± 2475	12 549 ± 491
LBD19-46	51.4780	−57.4756	75	28.3351	0.51864	4.63 ± 0.15	0.52 ± 0.04	50 202 ± 1883	10 632 ± 400
LBD19-74	53.8120	−60.1276	488	39.4430	0.51848	8.36 ± 0.26	0.53 ± 0.06	68 788 ± 2570	9618 ± 360
LBD19-75	53.8136	−60.1272	488	40.8886	0.51544	11.73 ± 0.26	0.53 ± 0.06	94 363 ± 3625	13 268 ± 511
LBD19-84	53.5438	−60.1463	65	13.1005	0.26170	3.39 ± 0.17	0.60 ± 0.09	37 259 ± 1919	7820 ± 404

The ^{10}Be ages were calculated with the 'LSDn' scaling scheme (Lifton et al., 2014), using the CRONUS-Earth online calculator version 3.0 (Balco et al., 2008; http://hess.ess.washington.edu/) and the production rate calculated with the NENA calibration data set of Balco et al. (2009). The ^{10}Be AMS standard applied was the ASTER in-house STD-11 with a ^{10}Be/^{9}Be ratio of 1.19×10^{-11} (Braucher et al., 2015) and a ^{10}Be half-life of 1.387 ± 0.012 Ma (Chmeleff et al., 2010; Korschinek et al., 2010). A constant thickness of 2 cm and a rock density of 2.65 g cm^{-3} was applied for all samples. No erosion and no topographic shielding were accounted for in our calculations. Snow cover corrections were not applied (Supporting Information). Asterisks (*) mark the samples that are considered as outliers and were not included in the mean age calculations (in bold). Numbers in parentheses includes the production rate uncertainty.

located on top of moraine crests, which are often wind-swept and thus probably prevented any significant snow accumulation (Supporting Information Table S2). Individual ^{10}Be exposure ages are presented with 1σ uncertainty (Table 1). Stated uncertainties are analytical only. Outliers were identified using the CRONUS-Earth online calculator and defined as ^{10}Be ages that are >2σ older or younger from the mean of the remaining ^{10}Be ages. Probability distribution function (PDF) plots were generated using the iceTEA (Tools for Exposure Ages from ice margins; http://ice-tea.org/en/) 'Import and plot ages' tool (Jones et al., 2019), in which the moraine ages were defined as the error-weighted mean of the sample population and the error-weighted internal uncertainty, excluding outliers. We include the production rate uncertainty in quadrature when comparing and discussing landform ages with independent climate records and radiocarbon ages. Additionally, ^{10}Be ages from Ullman et al. (2016) were recalculated using the same parameters as above to allow direct comparison with our new ^{10}Be ages (Supporting Information Table S3).

Radiocarbon dating

Accelerator mass spectrometry (AMS) radiocarbon dating was carried out on marine shells collected in 2019. The four obtained AMS ^{14}C ages were calibrated within the age–depth modelling process and converted to calendar

years using the online software Calib 8.2 (Stuiver & Reimer, 1993; http://calib.org/) with the Marine20 radiocarbon age calibration curve (Heaton et al., 2020). A local reservoir correction (ΔR) of −2 ± 69 was used to account for the regional offset of the world ocean ^{14}C age (McNeely et al., 2006). These four ages complement a dataset of 41 previously published ^{14}C ages that have also been recalibrated. Marine samples were calibrated using the aforementioned parameters, whereas terrestrial samples were calibrated using the IntCal20 radiocarbon age calibration curve (Reimer et al., 2020). All individual radiocarbon ages are presented as the mean of the calibrated age range with 1σ uncertainty (Table 2).

Retreat rates

The moraine map was used to reconstruct retreat rates of the LIS in easternmost Québec–Labrador. When ice-contact deposits were absent (i.e. west of Lake Melville), retreat isochrons of former ice margin positions (i.e. 7.9, 7.6 and 7.5 ka) were tentatively drawn perpendicular to the ice-flow direction where minimum limiting ages are available. Ice retreat rates were then calculated along time–distance transects perpendicular to the retreating ice margin. The transects were hand-drawn radially from the ~7.5-ka isochron of the LIS to the coast, where they are at intervals of ~50 km. This approach allowed each moraine system to be crossed at least three times, since no transect intersects all five mapped ice margin positions. The mean linear retreat rate was then calculated between every ice margin position using the ages for each moraine system presented in this paper for estimating the land-based ice margin retreat. These retreat rates represent minimum values as they do not take into account possible readvances of the LIS margin and their respective durations.

Table 2. Radiocarbon and calibrated radiocarbon ages from material collected in easternmost Québec–Labrador.

Laboratory ID	Latitude (DD)	Longitude (DD)	Dated material	^{14}C a BP ± 1σ	Cal a BP ± 1σ	Source
LBD19-62	53.5192	−60.1469	*Hiatella arctica*	8155 ± 15	8460 ± 45	This study
LBD19-61	53.5192	−60.1469	*Mya truncata*	8150 ± 20	8460 ± 50	This study
LBD19-81	53.5192	−60.1469	*Mya truncata*	8120 ± 20	8430 ± 50	This study
LBD19-79	53.2596	−60.3774	*Mya arenaria*	7875 ± 120	8160 ± 150	This study
AA-58969	54.6166	−56.1761	Shell fragment	12 060 ± 60	13 390 ± 120	Jennings et al., 2015
BETA-16518	51.4900	−56.9800	Walrus bone	11 650 ± 160	12 980 ± 180	Harington et al., 1993
GSC-2825	51.6806	−56.6999	*Mya truncata*	11 300 ± 140	12 650 ± 160	Lowdon and Blake, 1979
SI-3139	53.2333	−58.5500	Gyttja	10 650 ± 290	12 480 ± 380	Lamb, 1980
GSC-3022	52.4500	−56.5300	Silty gyttja	10 500 ± 140	12 380 ± 120	Engstrom and Hansen, 1985
GSC-3014	54.1200	−56.6800	Foraminifera	11 000 ± 220	12 270 ± 300	Vilks et al., 1984
GSC-4283	51.7500	−56.5100	Gyttja	10 400 ± 120	12 260 ± 220	Grant, 1992
UCI-45371	55.3017	−58.1485	*Nuculana* spp.	10 925 ± 25	12 240 ± 160	Dalton et al., 2020
GSC-4175	51.4900	−56.9800	*Mya arenaria*	10 800 ± 120	12 050 ± 240	Grant, 1992
BETA-19574	55.1300	−57.4700	Mixed shells	10 710 ± 170	11 900 ± 300	Dyke et al., 2003
BETA-11697	51.5000	−57.2500	Shell	10 470 ± 120	11 530 ± 220	Dyke et al., 2003
SI-3350	52.5200	−57.0300	Gyttja	9985 ± 145	11 520 ± 200	Lamb, 1980
SI-3137	51.5166	−57.3000	Gyttja	9920 ± 110	11 410 ± 90	Lamb, 1980
SI-3348	53.0500	−57.7500	Silty gyttja	9910 ± 120	11 400 ± 100	Lamb, 1980
GX-6345	55.0833	−59.1667	Foraminifera	10 275 ± 225	11 270 ± 360	Barrie and Piper, 1982
GSC-3067	52.2700	−58.0500	Gyttja	9740 ± 170	11 110 ± 160	Blake, 1982
AA-16750	54.6200	−56.1800	*Yoldiella* spp.	10 155 ± 80	11 090 ± 170	Andrews et al., 1999
GSC-1453	54.6750	−57.8083	*Serripes groenlandius*	9040 ± 230	9600 ± 320	Hodgson and Fulton, 1972
GSC-1453 (2 L)	54.6750	−57.8083	*Serripes groenlandius*	9030 ± 115	9570 ± 180	Hodgson and Fulton, 1972
WIS-1962	52.3000	−58.3700	Gyttja	8390 ± 80	9390 ± 45	King, 1985
WIS-1852	51.3170	−61.5100	Gyttja	8330 ± 110	9310 ± 110	King, 1985
WIS-1961	53.5800	−58.5800	Gyttja	8270 ± 80	9250 ± 100	King, 1985
GSC-1453 (1 L)	54.6750	−57.8083	*Serripes groenlandius*	8750 ± 150	9220 ± 200	Hodgson and Fulton, 1972
SI-1739	54.4000	−57.7167	Gyttja	8255 ± 400	9190 ± 480	Jordan, 1975
TO-200	53.7100	−59.5767	*Nuculana minuta*	8380 ± 90	8750 ± 170	Vilks et al., 1987
WIS-1850	52.3167	−60.3833	Gyttja	7620 ± 120	8420 ± 110	King, 1985
TO-1123	54.5500	−60.7833	*Nuculana* spp.	8080 ± 60	8380 ± 120	Awadallah and Batterson, 1990
WIS-1963	52.4500	−60.5667	Basal gyttja	7510 ± 80	8310 ± 50	King, 1985
GSC-2970	53.5250	−60.1500	*Balanus hameri*	8000 ± 100	8290 ± 150	Lowdon and Blake, 1980
BETA-28885	54.8167	−60.7333	*Portlandia*	7950 ± 90	8240 ± 140	Awadallah and Batterson, 1990
GSC-1254	53.2583	−60.7458	Pelecypod	7890 ± 150	8180 ± 180	Lowdon and Blake, 1975
TO-5695	55.2202	−61.2873	*Mesodesma arctatum*	7880 ± 70	8170 ± 120	Dyke et al., 2003
WIS-1855	53.0500	−61.4833	Gyttja	7150 ± 80	7970 ± 50	King, 1985
GSC-3661	52.3000	−62.1167	Gyttja	7080 ± 110	7890 ± 40	King, 1985
WIS-1960	53.2667	−62.4500	Lake sediments	6810 ± 100	7660 ± 90	King, 1985
WIS-1849	53.5000	−63.7000	Gyttja	6620 ± 110	7500 ± 80	King, 1985
GSC-3241	55.3333	−63.3000	Gyttja	6600 ± 100	7490 ± 80	Lamb, 1985
GSC-1592	54.0000	−62.9900	Mosses	6560 ± 200	7440 ± 180	Lowdon and Blake, 1973
GSC-3252	55.0330	−62.6330	Gyttja	6520 ± 150	7410 ± 110	Lamb, 1985
GSC-3640	52.5700	−63.6000	Gyttja	6050 ± 90	6910 ± 110	King, 1985
I-728	53.5800	−63.9500	Basal peat	5275 ± 250	6490 ± 240	Morrison, 1970

The AMS ^{14}C ages were calibrated within the age–depth modelling process, using the online software Calib 8.2 with the Marine20 (Heaton et al., 2020) and IntCal20 (Reimer et al., 2020) radiocarbon age calibration curves. A local reservoir correction (ΔR) of −2 ± 69 was used to account for the regional offset of the world ocean ^{14}C age, as determined by McNeely et al. (2006).

Results

^{10}Be ages and moraine systems

Moraine systems along the SE–NW transect of eastern Québec–Labrador are here briefly described. The resulting ^{10}Be ages from the sampled boulders and surfaces are provided for each of these moraine systems.

Three erratic boulders located above marine limit were sampled in the easternmost sector of the study area, where morainic landforms are sparse. These erratic boulders constrain a series of closely spaced recessional moraines that have not yet been linked to any major moraine system. Since the moraine ridges were mostly located below marine limit, three boulders –located on both sides– were selected to assess the timing of their formation; two 'coastal' boulders (LBD19-30 and LBD19-31) were located within 2 km of the coast and one 'inland' boulder (LBD19-28) was sampled ~40 km from the coast. The coastal erratic boulders provided ^{10}Be ages of 14.1 ± 0.6 and 12.5 ± 0.5 ka (Table 1), whereas the erratic boulder collected 40 km inland provided a ^{10}Be age of 12.0 ± 0.5 ka (Table 1).

The Brador Moraine consists of small-amplitude moraine ridges coinciding with the marine limit (~140 m) (Fig. 3A) and outwash deposits occupying lower areas in narrow valleys. Some moraine ridges show traces of local glaciotectonic deformation, indicating readvance of the ice margin before stabilization. Five boulders were sampled from three different segments of the Brador Moraine over a distance of ~75 km. These boulders yielded consistent ^{10}Be ages ranging between 12.6 ± 0.7 and 13.4 ± 0.5 ka and a weighted average of 12.9 ± 0.2 ka (Table 1; Fig. 4).

The Belles Amours Moraine consists of series of small sinuous ridges, each a few metres high and less than 20 m wide (Fig. 3B). This moraine system has a SW–NE orientation and is cross-cutting the Brador Moraine west of Blanc Sablon (Fig. 1). Five boulders were sampled from two of the main crests of the Belles Amours Moraine. They yielded ^{10}Be ages ranging from 11.2 ± 0.5 to 12.0 ± 0.4 ka (Table 1), resulting in a weighted average of 11.5 ± 0.3 ka (Fig. 4). Additionally, a bedrock surface sampled 4 km behind the Belles Amours Moraine and at 75 m above sea level (m.a.s.l.) –located below marine limit (~130 m.a.s.l.; Grant, 1992)– yielded an age of 10.8 ± 0.4 ka (LBD19-46; Table 1), indicating the emergence from marine waters and hence representing a minimum-limiting age constraint.

The Paradise Moraine consists of a 20-km-wide complex of glaciofluvial deposits pitted with kettles, as well as fields of hummocky and ribbed moraines (Fig. 3C). East of the Mealy Mountains, the moraine overprints glacial lineations at an odd angle, testifying to an ice flow reorganization that suggests an ice margin readvance. Five samples were collected on the Paradise Moraine and yielded a large range of ages from 11.4 ± 0.4 to 37.1 ± 1.2 ka (Table 1). Two samples yielded (too-) old ^{10}Be ages of 20.8 ± 0.7 and 37.1 ± 1.2 ka, while the three remaining samples have exposure ages ranging from 11.4 ± 0.4 to 12.7 ± 0.5 ka and a resulting weighted average of 12.1 ± 0.6 ka (Fig. 4).

The Little Drunken Moraine is located ~250 km inland from the coast. It has a lobate geometry and is defined by series of 5- to 40-m-high till ridges (Fig. 3D) associated with extensive outwash-plain deposits in proglacial valleys. Five samples were collected from the main crest of the Little Drunken Moraine: three samples yielded ^{10}Be ages ranging from 9.8 ± 0.4 to 11.3 ± 0.4 ka, with two ages at 13.5 ± 0.4 and 14.7 ± 0.5 ka considered as outliers (Table 1). The weighted average of the three remaining ages is 10.6 ± 0.7 ka (Fig. 4).

Two bedrock surfaces were sampled from the top of Mokami Hill (488 m.a.s.l.; Fig. 1) in order to assess ice thinning at the head of Lake Melville (LBD19-74 and LBD19-75). Although located <50 m apart, these sampled yielded disparate ^{10}Be ages of 10.0 ± 0.4 and 13.8 ± 0.5 ka (Table 1). Dating surfaces from the mountain top west of Lake Melville therefore remains inconclusive. The large span of ages (>3 ka) suggests that (i) at least one sample is unreliable, or (ii) they have endured differential erosion. Although it is likely that the older age is unreliable based on its location and nearby ages (i.e. the Sebaskachu Moraine), it is impossible to assess the actual exposure age of the mountain surface at this point and more samples should be collected to document the thinning of the LIS in the region during the early Holocene.

The Sebaskachu Moraine, located west of Lake Melville, consists of small linear moraines with well-defined narrow crests ~10 m high on the plateau (Fig. 3E); in valleys it consists of large (>50 m) subaqueous ice-contact depositional systems. Five boulders sampled from the Sebaskachu Moraine on the plateau yielded ^{10}Be ages ranging between 7.9 ± 0.3 and 9.1 ± 0.3 ka (Table 1). The weighted average of these five samples is 8.4 ± 0.4 ka (Fig. 4). Additionally, a boulder was sampled from the top of a valley moraine near Happy Valley-Goose Bay at 65 m.a.s.l. and yielded an age of 7.8 ± 0.4 ka (LBD19-84; Table 1). This site –located below marine limit (~135 m.a.s.l.; Fitzhugh, 1973)– provides the timing of the emergence rather than ice retreat. The regional relative sea-level curve from Fitzhugh (1973) suggests that the sample was shielded by the water column for up to 600 years. It therefore only provides a minimum estimate of the deglaciation, although adding these 600 years would closely match the weighted age calculated for the Sebaskachu Moraine.

Five samples were also collected 40 km west of Happy Valley–Goose Bay on minor moraine ridges (<3 m) in the Peter's River valley, above marine and lake limits. The samples yielded three ^{10}Be ages ranging from 7.5 ± 0.3 to 9.0 ± 0.4 ka, with two outliers at 6.8 ± 0.4 and 12.4 ± 0.5 ka (Table 1). The three remaining samples are, however, slightly disparate with a ^{10}Be weighted average age of 8.1 ± 0.5 ka (Fig. 4).

Radiocarbon ages

Three shell samples were collected in the southern extension of the Sebaskachu moraine, near Happy Valley-Goose Bay. These shells were embedded within the till composing the subaqueous ice-contact system, therefore possibly pre-dating readvance of the ice margin. These samples yielded consistent ages of 8.5 ± 0.1 cal ka BP (LBD19-62), 8.5 ± 0.1 cal ka BP (LBD19-61) and 8.4 ± 0.1 cal ka BP (LBD19-81). A shell collected in glaciomarine muds of the Churchill River bank 50 km west of the Sebaskachu Moraine yielded an age of 8.2 ± 0.2 cal ka BP (LBD19-79). Together, these results provide maximum and minimum limiting ages for the deposition of the Sebaskachu Moraine, which are in agreement with (i) former ^{14}C dating (Fig. 5; Table 2), and (ii) the cosmogenic exposure age of the Sebaskachu Moraine (8.4 ± 0.4 ka).

Discussion

Ice margin stabilizations in easternmost Québec–Labrador and regional correlations

The new cosmogenic exposure ages allow us to define the timing of deposition of the moraine systems of easternmost Québec–Labrador that record major readvance and/or stabilization stages of the LIS margin during its overall northwestward

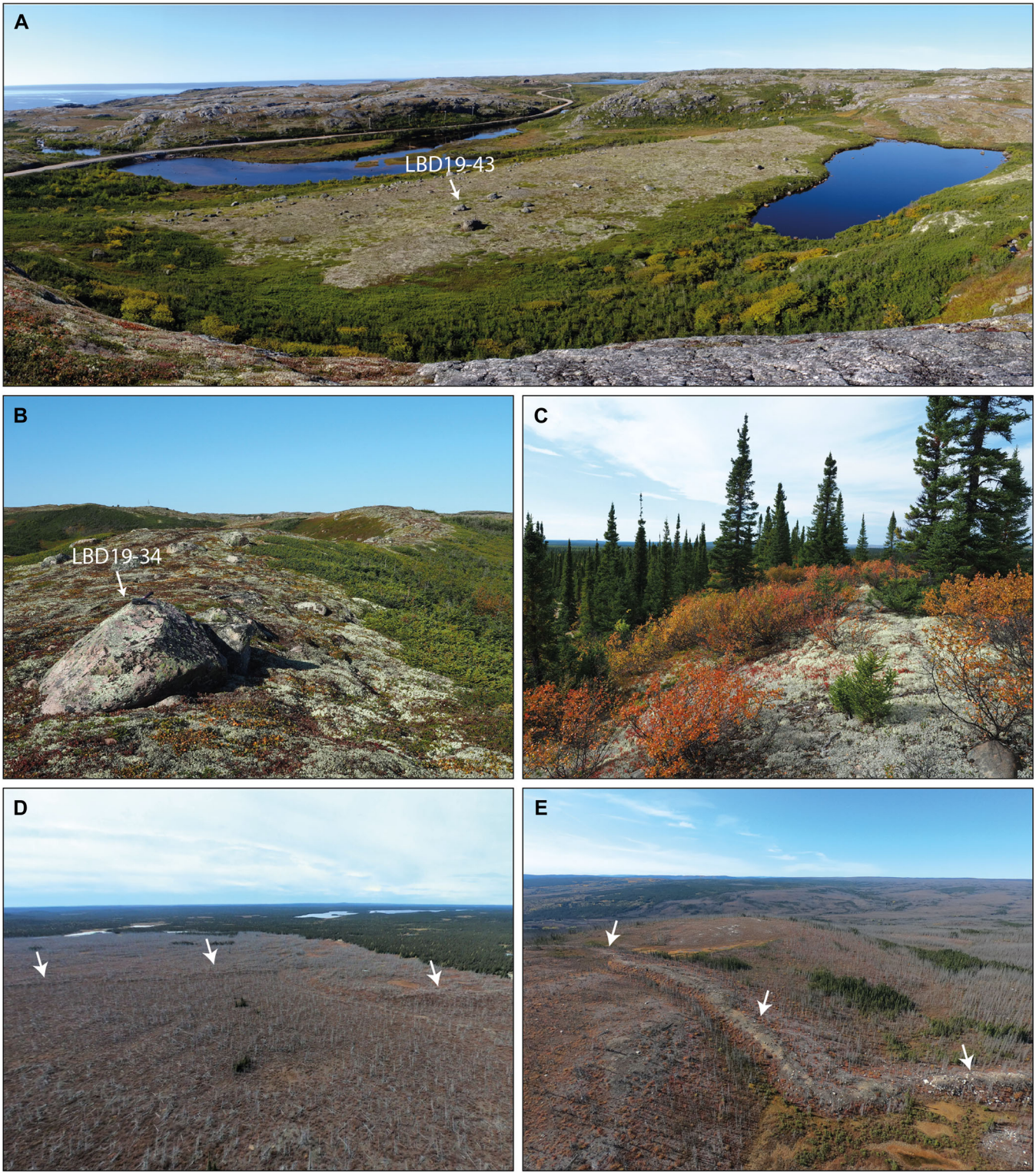

Figure 3. Photos of the major moraine systems of easternmost Québec–Labrador. (A) View of the Brador Moraine, with representative sample LBD19-43 (12.8 ± 0.5 ka). (B) View of the Belles Amours Moraine, with representative sample LBD19-34 (11.1 ± 0.5 ka). (C) View of the Paradise Moraine. (D) View of the Little Drunken Moraine (arrows). (E) View of the Sebaskachu Moraine (arrows). [Color figure can be viewed at wileyonlinelibrary.com]

retreat. These results are consistent and in chronological order in most cases, except for the Paradise Moraine that appears older than the Belles Amours Moraine deposited ~100–120 km to the east. The timing and correlations of the moraine systems are discussed below with respect to previously published data.

The age of the Brador Moraine system of 12.9 ± 0.7 ka (including the production rate uncertainty propagated through in quadrature) is supported by a robust ^{10}Be chronology and corresponds to the beginning of the YD chronozone. This age is further supported by a series of minimum-limiting radiocarbon ages ranging from 11.4 ± 0.1 to 12.2 ± 0.2 cal ka BP and maximum-limiting ages ranging from 12.7 ± 0.2 to 13.0 ± 0.2 cal ka BP (Fig. 5; Table 2). Additionally, the inland erratic boulder dated at 12.0 ± 0.5 ka, supported by a nearby age of 12.4 ± 0.1 cal ka BP (Engstrom & Hansen, 1985; Fig. 5; Table 2), suggests that the recessional moraine system located between the two erratic boulder sites ('coastal' and 'inland') may correspond to or slightly succeed the Brador Moraine. There is no indication, however, for its extension north of this sector, but it is highly probable that it is located beyond the

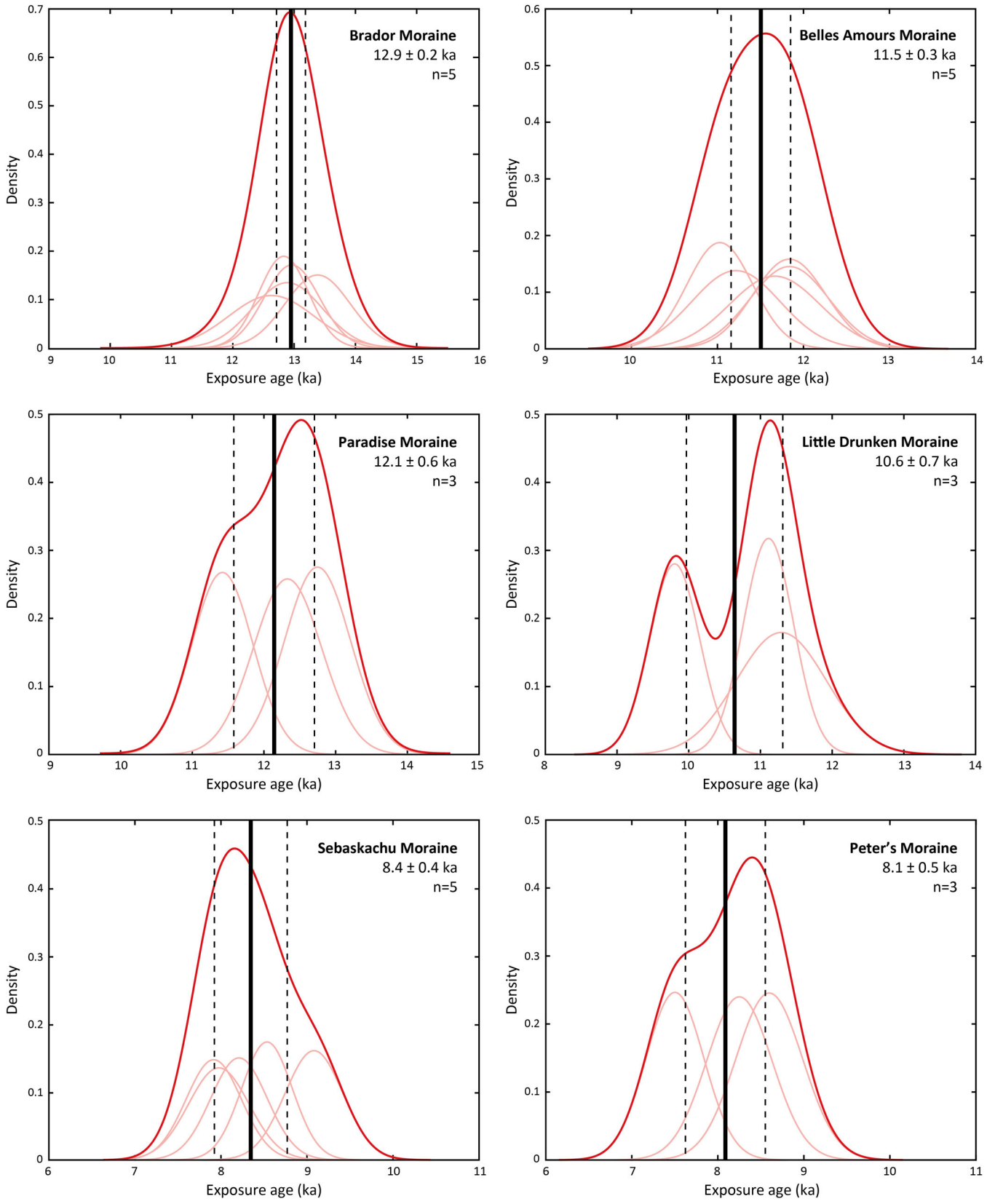

Figure 4. Probability distribution function (PDF) plots of ^{10}Be ages for moraine systems in easternmost Québec–Labrador, excluding outliers (see Results and Table 1). The black and dashed lines represent the weighted average and the 1σ interval. [Color figure can be viewed at wileyonlinelibrary.com]

coast of southeastern Labrador as foraminifera samples offshore yielded ages ranging from 11.1 ± 0.2 to 12.3 ± 0.3 cal ka BP (Table 2). Our results therefore suggest that the Brador Moraine is time-equivalent to the St-Narcisse Moraine in southern Québec (Occhietti, 2007) and possibly to one of the ice-contact grounding-zone wedge systems observed offshore the Québec North Shore region (Lajeunesse et al., 2019). It would also be contemporaneous with the Saglek Moraine located in the Torngats Mountains of northern Labrador (Clark et al., 2003). Consequently, the coastal erratic boulders suggest deglaciation of the coast of easternmost Québec–Labrador between 14.1 ± 0.6 and 12.5 ± 0.5 ka. Opening of the Belle Isle Strait

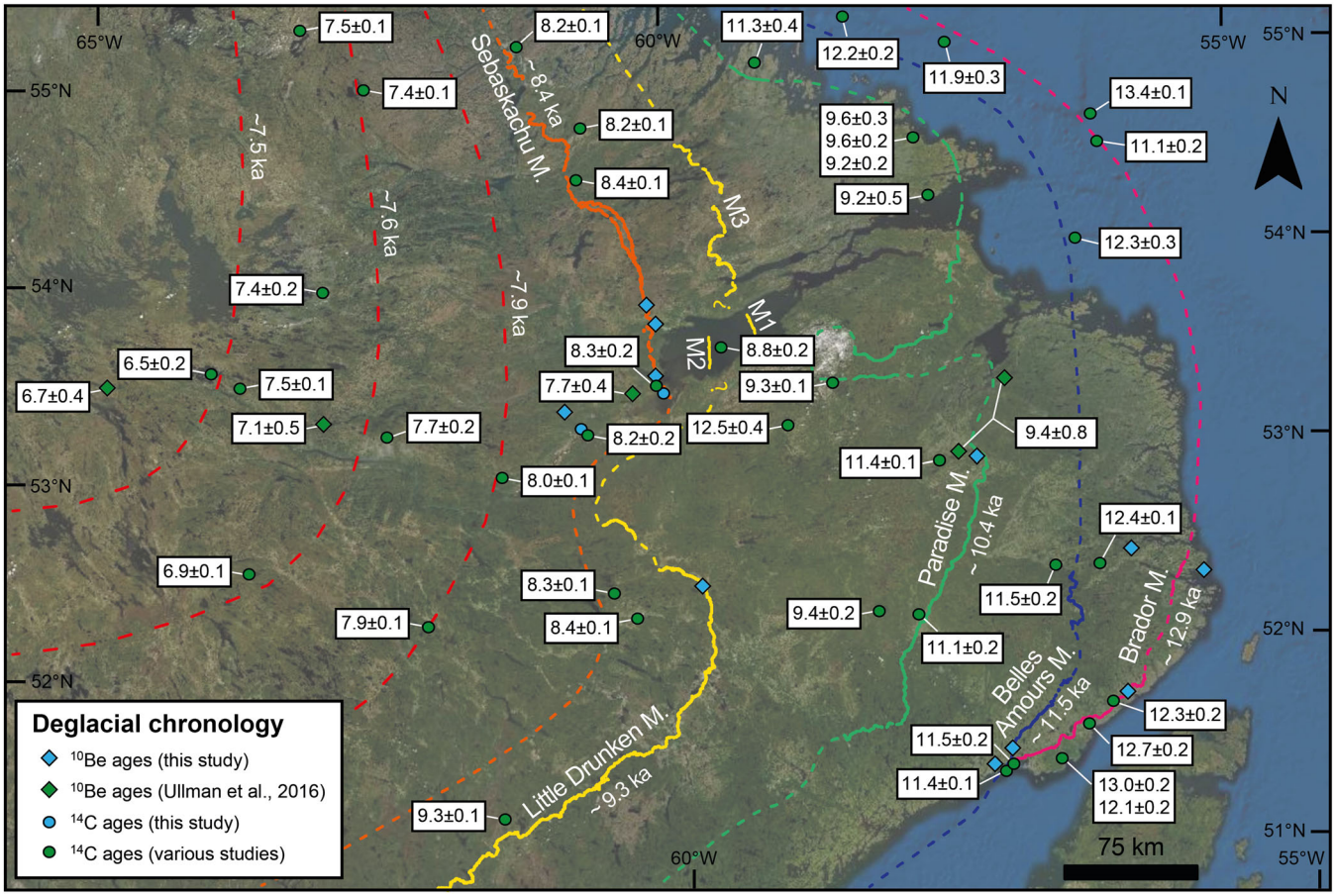

Figure 5. Previously published ages in easternmost Québec–Labrador. Cosmogenic ^{10}Be ages are recalculated from Ullman et al. (2016). Radiocarbon ^{14}C ages are compiled from various sources (Table 2). For ages from this study, the reader is referred to Fig. 1. All ages are reported in thousand years (ka). Full lines represent mapped moraines and dotted lines represent potential extension of these systems. Extension of the moraine systems and retreat isochrons of former ice margin positions (i.e. 7.9, 7.6 and 7.5 ka) were tentatively drawn based on available minimum- and maximum-limiting ages. [Color figure can be viewed at wileyonlinelibrary.com]

and isolation of the Newfoundland Ice Cap from the LIS therefore occurred prior to that timing, presumably during the Bølling–Allerød warm period (14.7–12.9 ka BP). This interpretation supports what has previously been proposed by Shaw et al. (2006) who argued that disconnection between the two ice masses occurred between 14.8 and 14.0 cal ka BP. In this scheme, the time frame proposed by Grant (1992) appears to be erroneous, as they argued that the opening of the Strait of Belle Isle and separation of the two ice masses occurred prior to 15 cal ka BP.

The age of 11.5 ± 0.7 ka for the deposition of the Belles Amours moraine ridges indicates a stabilization of the LIS margin at the beginning of the Holocene or near the end of the YD. This timing for the deposition of the Belles Amours moraine system contradicts the interpretation of Grant (1992) who argued that their deposition may have taken place only a few centuries after deposition of the Brador Moraine on the basis of only a minor relative sea-level fall between the two events. However, a relatively stagnant ice margin during the YD and a significant readvance –as evidenced by the cross-cutting relationship of the two moraines (Fig. 1)– may have significantly limited the rate of glacio-isostatic rebound in the region, similar to observations in Greenland during the Neoglacial ice expansion (Long et al., 2009). Although the mapped extent of this moraine is relatively limited (~100 km), the 12.0 ± 0.5 ka age of the inland erratic suggests that the ice margin was probably located west of this site at the time of deposition of the Belles Amours Moraine. Its northern extent can, however, only be tentatively mapped. Additionally, a basal lacustrine sample dated at 11.5 ± 0.2 cal ka BP (Lamb, 1980; Fig. 5; Table 2)–similar to the mean cosmogenic exposure age of the Belles Amours Moraine samples–may provide an indication for its approximate location near that site. The timing of deposition of the Belles Amours Moraine suggests a correlation with the Mars-Batiscan Moraine in southern Québec (Occhietti, 2007), although the physical connection between the two systems remains ambiguous. It is possible that the Belles Amours Moraine corresponds offshore to one of the youngest ice-contact grounding-zone wedges (Lajeunesse et al., 2019) and, onshore, to the Baie Trinité Moraine on the Québec North Shore (Fig. 1B; Occhietti et al., 2011). However, further dating would be needed to confirm the correlation as the timing of deposition of the Baie-Trinité Moraine is still not well constrained.

Direct dating of the Paradise Moraine remains inconclusive. Two of the samples yielded ages >20 ka, while the three remaining samples yielded an average age of 12.1 ± 0.9 ka. This age is stratigraphically problematic as it is older than the Belles Amours Moraine. Dated boulders located west of the Paradise Moraine system yielded a mean age of 10.4 ± 0.6 ka (Ullman et al., 2016) or 9.4 ± 0.8 ka when recalculated using the same parameters as for our ^{10}Be ages (Supporting Information Table S3; Fig. 5). Interestingly, four samples from Ullman et al. (2016) also yielded erroneous and largely too old ages (site CL1B in the original publication). The abundance of old ages implies that boulder recycling was important during deposition of the Paradise Moraine. However, it is uncertain where these boulders came from and when they were first

exhumed. Similarly, the dating of lake sediments, from about 50 km east of the moraine, yielded ^{14}C ages ranging up to >30 cal ka BP (Lamb, 1978) and were interpreted as the result of contamination by old carbon (King, 1985). These different occurrences of ages >20 ka suggest that the boulders sampled from the Paradise Moraine were affected by isotopic inheritance yielding artificially old and erroneous exposure ages. This isotopic inheritance points toward generally low glacial erosion rates and/or transport of supraglacial material on the plateau southwest of the Mealy Mountains. However, an age of 9.4 ± 0.1 cal ka BP (King, 1985; Fig. 5; Table 2) collected from basal lake sediments 20 km west of the moraine provides an indication for a later deglaciation. A moraine system located east of the Mealy Mountains correlates with the Paradise Moraine and corresponds to a lobe emanating from Lake Melville, leaving the summits of the Mealy Mountains deglaciated at that time. Radiocarbon dating of marine shells along a riverbank east of this moraine system yielded ages ranging from 9.2 ± 0.2 to 9.6 ± 0.3 cal ka BP (Hodgson & Fulton, 1972; Fig. 5; Table 2), which is in line with the exposure age retained for the abandonment of the Paradise Moraine at 9.4 ± 0.8 ka (recalculated from Ullman et al., 2016). Correlations with other sectors of the Québec–Labrador Ice Dome are challenging at this stage as the extension of the Paradise Moraine beyond the study area remains elusive.

The Little Drunken Moraine cosmogenic exposure ages also show a wide distribution with two outliers. These results should be interpreted with caution since they were also collected from a site on the plateau southwest of the Mealy Mountains; these samples were therefore potentially subject to isotopic inheritance similarly to the Paradise Moraine samples. Nonetheless, the resulting weighted mean of 10.6 ± 1.0 ka matches the ^{14}C ages for the Québec North Shore Moraine, which has been previously mapped as the southwestern extension of the Little Drunken Moraine (Dubois & Dionne, 1985; Dietrich et al., 2019). In turn, recent cosmogenic dating of the Québec North Shore Moraine suggested a ^{10}Be age of 9.2 ± 0.5 ka for its abandonment (Ullman et al., 2016). Recalculation of these ages again gives an even younger moraine age of 8.5 ± 0.7 ka. Regardless of the calculation method, ages from Ullman et al. (2016) are consistent with a radiocarbon age of 9.3 ± 0.1 cal ka BP (King, 1985; Fig. 5; Table 2) collected from the base of a lacustrine record located less than 10 km northwest of the Little Drunken Moraine. The extension of the moraine is arguably represented across Lake Melville either on seismic data (Fig. 1C–M1; Syvitski & Lee, 1997) or on swath bathymetry imagery (Fig. 1C–M2; Gebhardt et al., 2020). Which of these two moraines represents the Little Drunken Moraine is unclear as the physical connection between these systems is missing. The connection with an unnamed moraine system located north of Lake Melville (Fig. 1C–M3) –interpreted to be equivalent to the Little Drunken Moraine by Batterson et al. (1987)– is also absent. However, a minimum-limiting age of 8.8 ± 0.2 cal ka BP (Vilks et al., 1987; Fig. 5; Table 2) on shells in Lake Melville indicates that the ice margin probably extended across the lake at the time of the deposition of the Little Drunken Moraine. To the north, a moraine system of similar age (Tasiuyak Moraine–9.3 cal ka BP) reported in the Nain–Okak region could represent the northern extension of the ice margin at the time of deposition of the Little Drunken Moraine (Andrews, 1963; Recq et al., 2020).

Cosmogenic exposure dating of the Sebaskachu Moraine yielded an age of 8.4 ± 0.6 ka, which is in strong agreement with the radiocarbon ^{14}C ages (<8.4 ± 0.1 and >8.2 ± 0.2 cal ka BP; Table 2) bracketing the moraine formation age. A shell collected in deglacial deposits on top of the moraine near Happy Valley-Goose Bay further supports abandonment of the Sebaskachu Moraine by 8.3 ± 0.2 cal ka BP (Lowdon & Blake, 1980; Table 2). Additionally, shells collected from three ice-contact deltas north of our sample site yield ages of 8.4 ± 0.1, 8.2 ± 0.2 and 8.2 ± 0.1 cal ka BP (Fig. 5; Table 2). As these deltas are all located downstream from lakes, it is unlikely that their deposition correspond to stabilization of the ice margin further inland. These ages confirm the northern extension of the Sebaskachu Moraine up to the Adlatok Valley, where a ~20-km gap remained in the moraine mapping (Fig. 1 C). The southern extension of the moraine remains undefined, but minimum-limiting radiocarbon ages of 8.4 ± 0.1 and 8.3 ± 0.1 cal ka BP (King, 1985; Fig. 5; Table 2) collected in lake sediments suggest that the ice margin at that time was probably located ~50 km west of the Little Drunken Moraine. The age of the Sebaskachu Moraine corresponds to the timing of deposition of the extensive Sakami Moraine in western Québec (Hillaire-Marcel et al., 1981; Hardy, 1982; Lajeunesse & Allard, 2003; Lajeunesse & St-Onge, 2008; Ullman et al., 2016) and the Cockburn moraines on Baffin Island (Bryson et al., 1969; Andrews & Ives, 1978; Dyke, 1979; Miller, 1980; Briner et al., 2007; Young et al., 2012).

The Peter's Moraine exposure age of 8.1 ± 0.7 ka is comparable to a nearby site from Ullman et al. (2016), which gave an age of 7.7 ± 0.4 ka. The moraine age is similar to the age of 8.2 ± 0.2 cal ka BP on a shell collected in glaciomarine deposits along the Churchill River (Fig. 1; Table 2). It is also coeval with another shell collected in a nearby outcrop that yielded an age of 8.2 ± 0.4 cal ka BP (Lowdon & Blake, 1975; Fig. 5; Table 2). As a minor moraine system partly controlled by topographic features, it is unlikely that correlations can be made with other systems of the Québec–Labrador Ice Dome. It probably represents subordinate recessional moraines from the Sebaskachu Moraine located ~30 km to the east, as suggested by the short time interval (<0.3 ka) separating both landforms.

To summarize, while the Brador, Belles Amours and Sebaskachu moraines are particularly well dated at ~12.9, ~11.5 and ~8.4-8.2 ka respectively, the age of the Paradise and Little Drunken moraines remains uncertain. In addition, published cosmogenic exposure ages (Ullman et al., 2016) and recalibration of legacy radiocarbon ages (King, 1985) for the deglaciation west of Lake Melville allow us to refine later positions of the LIS margin for the interior of Québec–Labrador up to Churchill Falls and allow us to estimate the associated retreat rates for that period. A radiocarbon age indicates that the ice margin was located at the head of the Churchill River valley by 8.0 ka (King, 1985; Fig. 5; Table 2). Cosmogenic exposure ages (Ullman et al., 2016) and radiocarbon ages (King, 1985) indicate that the ice margin retreated rapidly to Lake Winokapau by ~7.6 ka and to Churchill Falls by ~7.5 ka (Fig. 5; Table 2).

Ice-sheet response to abrupt climatic forcings

Controls on the formation of the Brador, Belles Amours and Sebaskachu moraines, which yield robust ages (Fig. 4), are first investigated in this discussion. The significance of the Paradise and Little Drunken moraines, less well dated, need further discussion as their timing remain uncertain.

The occurrence of the Brador Moraine (12.9 ± 0.7 ka) roughly outlining the marine limit (~140 m.a.s.l.) along the coast of easternmost Québec–Labrador was speculated as representing a mass balance readjustment (re-equilibration) of the LIS when the calving ice margin reached the Brador highlands following disconnection from the Newfoundland Ice Cap (Grant, 1992). The role of the topography in stabilizing marine-based ice margins has been extensively discussed in recent literature (e.g. Jamieson et al., 2012; Batchelor et al., 2019; Brouard & Lajeunesse, 2019). However, this role

appears to be secondary in this particular situation as the moraine is also observed on the plateau between valleys. Although it is difficult to deny the role played by the transition from marine- to land-based in stabilizing the ice margin, it probably reflects an equilibrium state sufficient for stabilization following a readvance –evidenced by glaciotectonic deformation– triggered by the sudden decrease in temperature by 2°C (Fig. 6; Rasmussen et al., 2014) at the beginning of the YD (12.9–11.7 ka BP).

The age of the Belles Amours Moraine (11.5 ± 0.7 ka) suggests that it corresponds to the Preboreal Oscillation (11.5–11.3 ka BP), which is outlined by a sharp fall in temperatures in Greenland ice cores at the beginning of the Holocene (Fig. 6; Kobashi et al., 2017). Freshwater input into the North Atlantic by abrupt glacial lake drainages is postulated to have provoked alteration of the AMOC that resulted in several prominent early Holocene abrupt cooling events, including the Preboreal Oscillation, the 9.3-ka event and the 8.2-ka event (Barber et al., 1999; Fisher et al., 2002; Alley & Ágústsdóttir, 2005; Fleitmann et al., 2008). These freshwater inputs are expressed in the Labrador Sea as detrital carbonate peaks (DCPs) associated with a high concentration of ice-rafted debris (Jennings et al., 2015). In the case of the Preboreal oscillation, it is considered to have been triggered by drainage of the glacial Lake Agassiz via the Mackenzie River (Fisher et al., 2002; Süfke et al., 2022) and corresponds in time with DCP 1 (Fig. 6; Jennings et al., 2015).

The Sebaskachu (8.4 ± 0.6 ka) and Peter's (8.1 ± 0.7 ka) moraine ages correspond closely to the well-known 8.2-ka cooling event recorded in various sediment cores in the North Atlantic region (Barber et al., 1999; von Grafenstein et al., 1998; Jennings et al., 2015; Kleiven et al., 2008) and ice cores of the Greenland Ice Sheet (Rasmussen et al., 2014). This cooling event is widely considered to be caused by the drainage of glacial Lake Agassiz–Ojibway into the North Atlantic via the Hudson Strait (e.g. Barber et al., 1999; Clarke et al., 2004; Lajeunesse & St-Onge, 2008; Brouard et al., 2021). Moraine crests in the vicinity of Peter's Moraine are minor and may as well be topographically controlled, and hence climatically insignificant, recessional features. Nonetheless, the close occurrence of both moraines has a clear temporal coincidence with the abrupt cooling event related to the collapse of the LIS over Hudson Bay at 8.2 ka and recorded in the Labrador Sea as DCP 7 (Fig. 6; Jennings et al., 2015). However, the timing of the Sebaskachu Moraine at the start of this event could also support the hypothesis of a broader cooling perturbation beginning at ~8.6 ka BP (Rohling & Pälike, 2005; Morrill et al., 2013) as a response to the early opening of the Tyrell Sea (Fig. 6; Jennings et al., 2015).

In view of the tightly clustered individual ($n = 5$) ages for the Belles Amours Moraine centred at 11.5 ± 0.3 ka, the ^{10}Be ages for the Paradise (12.1 ± 0.6 ka) and Little Drunken (10.6 ± 0.7 ka) moraines reported here are unlikely as they are unquestionably too old. Based on their stratigraphic position, the Belles Amours Moraine is expected to be older than the Paradise Moraine and, consequently, significantly older than the Little Drunken Moraine. To cope with these discrepancies, published cosmogenic exposure ages (Ullman et al., 2016) were incorporated in our age model. Their recalculations show ages of 9.4 ± 0.8 and 8.5 ± 0.7 ka for the Paradise Moraine and Québec North Shore-Little Drunken Moraine, respectively (see Supporting Information Table S3). While there are discrepancies between the ages from the original publication and our recalculations, the uncertainties still overlap between datasets. However, two key parameters could partly explain the younger ages of the samples in regard to the actual targeted landforms: (i) Ullman et al. (2016) sampled boulders sometimes located well behind morainic crests (up to 25 km), therefore systematically minimizing the moraine ages; and (ii) some samples were collected below the reported marine limit of 150 m (Carlson, 2020) for the site CL1, consequently delaying their exposure ages by a few centuries. These ages, representing minimum values for the abandonment of the moraines, are nonetheless coherent with minimum-limiting radiocarbon ages in the region and, consequently, complete our dataset without any chronological overlap between moraine segments. Combining both datasets could therefore allow the correlation of the Paradise Moraine to the 10.3-ka event and the Little Drunken Moraine to the 9.3-ka event, as suggested by Ullman et al. (2016). While the cause of the 10.3-ka cooling event remains elusive, its consequences, recorded by (i) the presence of DCP 2 (Fig. 6; Jennings et al., 2015) and (ii) the widespread stabilization of the ice margins in western Greenland and eastern Canada (Young et al., 2020a, 2021) are unequivocal and a correlation with the major Paradise Moraine is most likely. The 9.3-ka event, which is correlated to DCP 3 or 4 (Fig. 6; Jennings et al., 2015), was speculated to have been triggered either by the Noble Inlet readvance across Hudson Strait (Jennings et al., 2015) or a meltwater outburst flow from Lake Superior (Yu et al., 2010). This abrupt cooling event has been recorded around Baffin Bay as a widespread ice margin stabilization event (e.g. Lesnek & Briner, 2018; Crump et al., 2020; Young et al., 2020a) and may therefore correlate with the timing of deposition of the Little Drunken Moraine. The occurrence of two stabilizations in Lake Melville (M1, M2–Fig. 1C) could in fact correspond to the two DCP peaks observed around that event, if the moraine system identified on seismic data (M1) could be the result of a drawdown of the ice as speculated by several authors (i.e. Fulton & Hodgson, 1979; Vilks et al., 1987). This drawdown into Lake Melville may have provoked only a localized stabilization, although its occurrence elsewhere remains to be determined.

Finally, the compilation of cosmogenic exposure ages presented here, together with previously published cosmogenic and radiocarbon ages, identifies margin stabilizations and/or readvances of the eastern fringe of the LIS at ~12.9, ~11.5, ~10.4, ~9.3 and ~8.4–8.2 ka. This comprehensive ^{10}Be-based chronology clearly demonstrates that the timing of moraine deposition in easternmost Québec–Labrador was coeval with cold climatic events recorded in Greenland ice cores (Fig. 6), indicating that the LIS margin was interconnected with climate fluctuations at least regionally. The synchronicity of moraine deposition along the eastern fringe of the LIS from Baffin Island to southern Québec –that connect both continental- and marine-based segments of the ice margin– suggests strongly that readvances of the ice margin were triggered by major, short-term regional climatic deteriorations rather than by a mechanical adjustment or re-equilibration of the ice sheet (Hillaire-Marcel et al., 1981; Dubois & Dionne, 1985; Clark et al., 2000). This deglaciation chronology supports results from around Baffin Bay suggesting that early Holocene ice margin readvances and/or stabilizations of the LIS –and Greenland Ice Sheet– were caused by meltwater pulses into the Labrador Sea (Young et al., 2020a, 2021). Similar to their interpretation, detrital carbonate peaks from the Cartwright Saddle on the Labrador Shelf (Jennings et al., 2015) preceding the stabilizations/readvances of the ice margin in easternmost Québec–Labrador possibly indicate that abrupt cold reversals of the early Holocene were strongly influenced by meltwater pulses weakening the AMOC. While early Holocene cooling events appear to be triggered by freshwater input –often caused itself by abrupt lake drainage– into the Atlantic Ocean and recorded by detrital carbonate events in the Labrador Sea, further investigation should focus on identifying trigger mechanisms for such freshwater outbursts. The 1000- to 1200-year cyclicity behind those cooling events may suggest an external

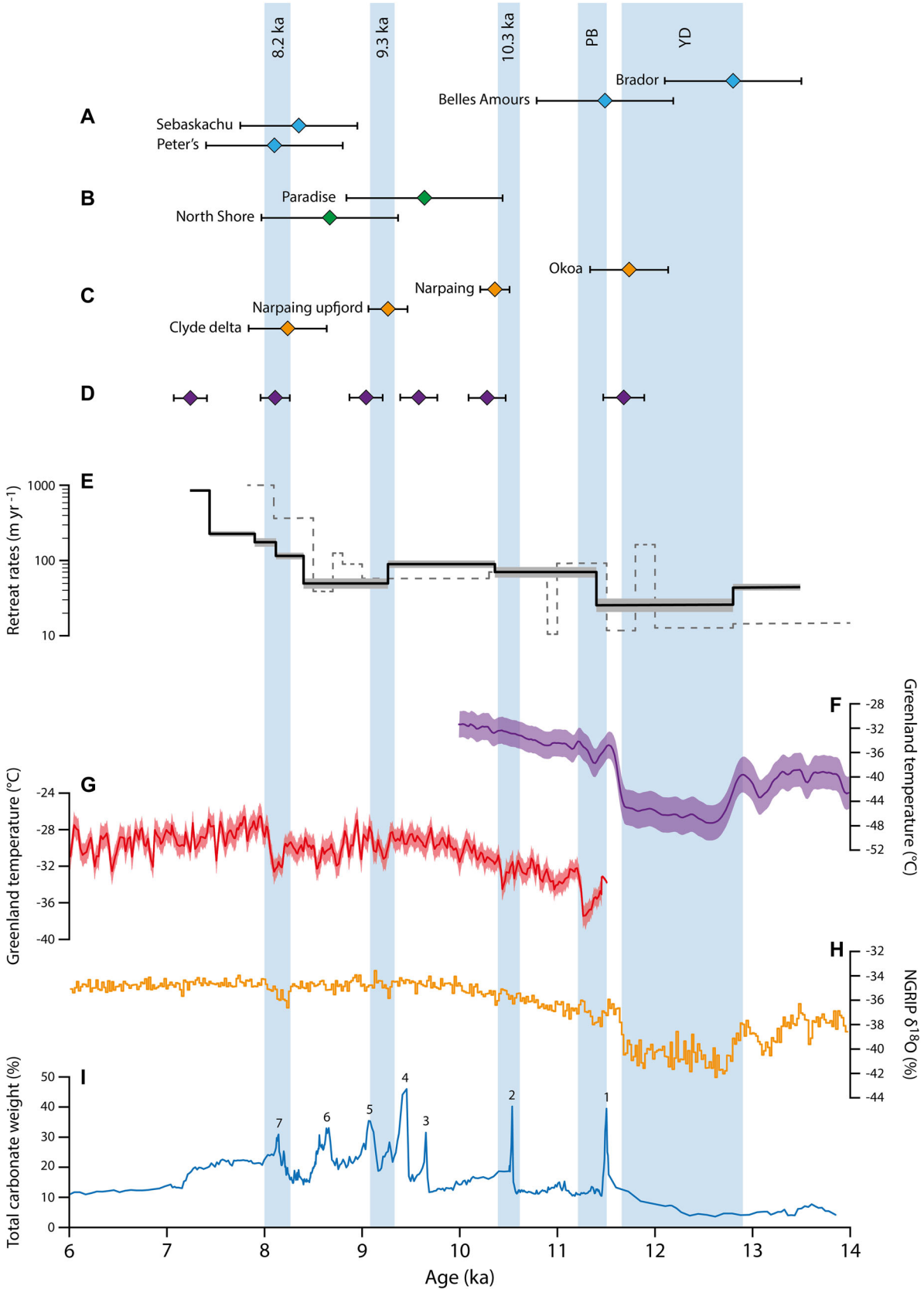

Figure 6. (A) Exposure ages of moraine systems of easternmost Québec–Labrador from this study. (B) Exposure ages of moraine systems of Labrador and Québec from Ullman et al. (2016). (C) Exposure ages of moraine systems of LIS outlet glaciers on Baffin Island from Young et al. (2020a). Additionally, we used one site from Briner et al. (2007) and recalculated in Young et al. (2013). (D) Composite record of Baffin Bay moraine deposition, from Young et al. (2021). (E) Average retreat rates in southern Labrador reconstructed from this study (black line) with the standard error of the mean (shading). Dashed dark grey line is from Dalton et al. (2020). Note that retreat rates are represented in a logarithmic scale. (F) Greenland mean-annual temperatures reconstructed using gas-phase $\delta^{15}N\text{-}N_2$ measurements (purple – ±1σ; Buizert et al., 2014). (G) Greenland mean-annual temperatures reconstructed using gas-phase $\delta Ar\text{-}N_2$ measurements (red – ±2σ; Kobashi et al., 2017). (H) $\delta^{18}O$ record from NGRIP project (orange; Rasmussen et al., 2014). (I) Total carbonate weight chronology in core MD99-2236 collected on the Labrador Shelf (blue; Jennings et al., 2015; Fig. 1). Vertical bars represent cold intervals discussed in the text. YD: Younger Dryas; PB: Preboreal. [Color figure can be viewed at wileyonlinelibrary.com]

forcing that influenced the rapid retreat of the ice margin prior to these events, thus favouring meltwater outburst. First proposed by Denton & Karlén (1973) –and later advocated by Bond et al. (1997)– the cyclicity of Holocene cooling events has been for decades very puzzling to researchers. Bond-like events, speculated by some to be influenced by enhanced solar activity (e.g. Bond et al., 2001), may certainly still be relevant to identify a source for such cycles, although their occurrence may as well simply be the result of several trigger mechanisms (Young et al., 2021).

Retreat rates reflect long-term climatic trends

Retreat rates across the study area probably reflect long-term (centennial- to millennial-scale) climatic trends, with minimum recession during colder periods and increasing rates corresponding to increasing temperatures. Minimum recession rates of the LIS margin in easternmost Québec–Labrador were observed during the YD (~25 m a^{-1}) and again between 9.3 and 8.2 ka (~50 m a^{-1}). The YD was marked by significantly lower temperatures over a relatively long period of ~1200 years (Fig. 6; Buizert et al., 2014), therefore contributing to a significant slowdown in ice retreat. A similar assessment could be made for the period between 9.3 and 8.2 ka, when another significant reversal in the warming temperature trend is observed (Fig. 6; Kobashi et al., 2017). Increasing retreat rates across the study area from 11.5 to 9.3 ka (75–90 m a^{-1}) could be linked to the warming climatic trend recorded in Greenland ice cores (Fig. 6; Kobashi et al., 2017). Collapse of the LIS can be recorded after 8.2 ka –regardless of climatic trend– as retreat rates started increasing drastically, reaching up to 1,000 m a^{-1} by 7.5 ka (Fig. 6).

Several lines of explanation can be invoked to explain the collapse of the LIS in central Québec–Labrador: (i) rapidly increasing temperatures in the Arctic and subarctic regions –similar to present-day observations– directly affecting its accumulation zone and resulting in negative mass balance (Carlson et al., 2009); or (ii) the Québec–Labrador Ice Dome reached a tipping point from which it was no longer in balance with climate and sustainable under early Holocene climatic conditions. Recurrent climatic cooling phases provoked by meltwater discharge events were suggested to have helped 'artificially' sustain the Québec–Labrador Ice Dome during the early Holocene (Ullman et al., 2016). In this perspective, it is possible that the absence of such events after 8.2 ka favoured the collapse of the LIS as a lagged response to the overall Holocene warming trend (Shakun et al., 2012; Buizert et al., 2014). With a constant negative mass-balance at the time, the Québec–Labrador Ice Dome eventually disappeared by 6 ka (Richard et al., 1982; Clark et al., 2000; Jansson, 2003; Occhietti et al., 2011; Dubé-Loubert et al., 2018).

However, it can be stressed that calculating retreat rates between stabilizations of the ice margin is only tentative in this situation, smoothing inappropriately the signal of ice-sheet readvances. Therefore, using an approach integrating estimates of hiatus duration (e.g. Lowell et al., 2021) would be more appropriate in order to exclude uncertainties related to the length of stabilizations and magnitude of potentially preceding readvances. However, this method would require further dating to better constrain the timing of the ice margin readvances and duration of the stabilizations.

Conclusion

This paper reports on 37 new cosmogenic ^{10}Be and four new radiocarbon ages in easternmost Québec–Labrador that allow us to establish a chronological framework of major moraine systems deposited during stabilizations/readvances stages of the LIS margin. These results improve the deglaciation history drawn for the region by earlier workers and document periods of regional ice margin stabilization at ~12.9, ~11.5, ~10.4, ~9.3 and ~8.4–8.2 ka. The combined ages outline a close relationship between climate and glaciodynamics of the LIS margin during the late Wisconsinan–early Holocene transition and are in line with previous work on Baffin Island and western Greenland suggesting that glacial dynamics were controlled by abrupt climatic events and possibly synchronous along the margin of entire ice sheets. The physical connection between the easternmost Québec–Labrador moraines and other systems of the eastern fringe of the LIS remains, however, ambiguous. Although correlations can be made with major moraine systems of southern Québec, large geographical gaps and chronological uncertainties persist. The transition between a land- to marine-based ice margin makes it difficult to accurately connect undated moraines from one region to another without a complete swathe of bathymetric coverage offshore.

Future work focusing on connecting the easternmost Québec–Labrador moraine systems with those of the Québec North Shore and northern Labrador is needed to provide a larger-scale palaeogeographical perspective of the major stages of the LIS margin in a period of rapid climatic fluctuations across a wide range of latitudes, as well as marine to continental contexts. Further direct dating is needed on moraine systems across the Québec–Labrador region to assess more precisely the extent of the LIS and the final stages of deglaciation at the YD–early Holocene transition. A better chronological constraint would not only be essential for future empirical-based numerical modelling assessing the contribution of the LIS to global sea-level changes, but it would also greatly increase our understanding of abrupt climatic cooling events induced by ice sheet-derived meltwater discharge into the North Atlantic. Although an almost consistent cyclical pattern of ~1000–1200 years is observed between the major ice margin stabilizations reported here during the early Holocene, the origin of these events as negative feedback triggered by meltwater inputs into the North Atlantic has yet to be explored as an analogue to potential forthcoming climate variation.

Acknowledgments. This project was funded by the ArcticNet Network of Centers of Excellence, Natural Sciences and Engineering Council of Canada (NSERC) and Sentinelle Nord (Apogée Canada) grants to P.L., Institut de Physique du Globe de Strasbourg (IPGS) grants to J.F.G., as well as Université de Strasbourg and Fondation Famille Choquette grants to P.O.C. We are thankful to the Centre d'études nordiques (CEN), Polar Knowledge Canada (POLAR) and SYSTER research programme from the CNRS-INSU for financial support during fieldwork. The French national AMS facility ASTER (CEREGE) is supported by the INSU/CNRS, the French MESR, and the CEA institute. We are thankful to G. Aumaître and K. Keddadouche for the AMS measurements. We thank Charles Brionne, Etienne Brouard and Vincent Rinterknecht who provided helpful comments on a previous draft of the paper. The manuscript was also greatly improved by fruitful discussions with Olivier Bourgeois, Colm Ò Cofaigh and Daniel Praeg, as well as formal reviews by Nicolás E. Young and one anonymous reviewer.

Funding. Canada First Research Excellence Fund, Natural Sciences and Engineering Research Council of Canada, Polar Knowledge Canada.

Conflict of interest—The authors declare that they have no known competing financial interests or personal relationships that could have appeared to influence the work reported in this paper.

Data availability statement

The data that support the findings of this study are available from the corresponding author upon reasonable request.

Supporting information

Additional supporting information may be found in the online version of this article at the publisher's web-site.

Table S1. ^{10}Be exposure ages corrected for elevation changes.

Table S2. ^{10}Be exposure ages corrected for snow cover.

Table S3. Recalculated ^{10}Be exposure ages from Ullman et al. (2016).

Abbreviations. AMOC, Atlantic Meridional Overturning Circulation; AMS, accelerator mass spectrometry; ASTER, Accélérateur pour les Sciences de la Terre, Environnement, Risques; CEREGE, Centre Européen de Recherche et d'Enseignement en Géosciences de l'Environnement; DCP, detrital carbonate peak; LGM, Last Glacial Maximum; LIS, Laurentide Ice Sheet; NENA, Northeastern North America; YD, Younger Dryas.

References

Alley, R.B., Mayewski, P.A., Sowers, T., Stuiver, M., Taylor, K.C. & Clark, P.U. (1997) Holocene climatic instability: a prominent, widespread event 8200 yr ago. *Geology*, 25(6), 483–486.

Alley, R. & Ágústsdóttir, A.M. (2005) The 8k event: cause and consequences of a major Holocene abrupt climate change. *Quaternary Science Reviews*, 24(10–11), 1123–1149.

Andrews, J.T. (1963) End moraines and late-glacial chronology in the northern Nain-Okak section of the Labrador coast. *Geografiska Annaler*, 45(2–3), 158–171.

Andrews, J.T., Keigwin, L., Hall, F. & Jennings, A.E. (1999) Abrupt deglaciation events and Holocene palaeoceanography from high-resolution cores, Cartwright Saddle, Labrador Shelf, Canada. *Journal of Quaternary Science*, 14(5), 383–397.

Andrews, J.T. & Ives, J.D. (1978) "Cockburn" Nomenclature and the Late Quaternary History of the Eastern Canadian Arctic. *Arctic and Alpine Research*, 10(3), 617–633.

Awadallah, S.A. & Batterson, M.J. (1990) Comment on "Late Deglaciation of the Central Labrador Coast and Its Implications for the Age of Glacial Lakes Naskaupi and McLean and for Prehistory," by P. U. Clark & W. W Fitzhugh. *Quaternary Research*, 34(3), 372–373.

Axford, Y., Briner, J.P., Miller, G.H. & Francis, D.R. (2009) Paleoecological evidence for abrupt cold reversals during peak Holocene warmth on Baffin Island, Arctic Canada. *Quaternary Research*, 71(2), 142–149.

Balco, G., Stone, J.O., Lifton, N.A. & Dunai, T.J. (2008) A complete and easily accessible means of calculating surface exposure ages or erosion rates from 10Be and 26Al measurements. *Quaternary Geochronology*, 3(3), 174–195.

Balco, G., Briner, J., Finkel, R.C., Rayburn, J.A., Ridge, J.C. & Schaefer, J.M. (2009) Regional beryllium-10 production rate calibration for late-glacial northeastern North America. *Quaternary Geochronology*, 4(2), 93–107.

Balco, G. (2020) Glacier change and paleoclimate applications of cosmogenic-nuclide exposure dating. *Annual Review of Earth and Planetary Sciences*, 48, 21–48.

Barber, D.C., Dyke, A., Hillaire-Marcel, C., Jennings, A.E., Andrews, J.T., Kerwin, M.W. et al. (1999) Forcing of the cold event of 8,200 years ago by catastrophic drainage of Laurentide lakes. *Nature*, 400(6742), 344–348.

Barrie, C.Q. & Piper, D.J. (1982) Late Quaternary Marine Geology of Makkovik Bay, Labrador. Geological Survey of Canada, Paper 81–17, 37 p.

Batchelor, C.L., Dowdeswell, J.A., Rignot, E. & Millan, R. (2019) Submarine Moraines in Southeast Greenland Fjords Reveal Contrasting Outlet-Glacier Behavior since the Last Glacial Maximum. *Geophysical Research Letters*, 46, 3279–3286.

Batterson, M.J., Scott, S. & Simpson, A. (1987) Quaternary mapping and drift exploration in the eastern part of the Central Mineral Belt. Labrador. *Current Research. Newfoundland Department of Mines and Energy, Mineral Development Division, Report*, 87–1.

Bierman, P.R., Caffee, M.W., Davis, P.T., Marsella, K., Pavich, M., Colgan, P. et al. (2002) Rates and timing of earth surface processes from in situ-produced cosmogenic Be-10. *Reviews in Mineralogy and Geochemistry*, 50(1), 147–205.

Blake Jr., W. (1956) Landforms and topography of the Lake Melville area, Labrador, Newfoundland. *Canada Department of Mines and Technical Surveys Geographical Bulletin*, 9, 93–97.

Blake, W. (1982) Geological Survey of Canada Radiocarbon Dates XXII. Geological Survey of Canada, Paper 82–7, 22 p.

Bond, G., Showers, W., Cheseby, M., Lotti, R., Almasi, P., DeMenocal, P. et al. (1997) A pervasive millennial-scale cycle in North Atlantic Holocene and glacial climates. *Science*, 278(5341), 1257–1266.

Bond, G., Kromer, B., Beer, J., Muscheler, R., Evans, M.N., Showers, W. et al. (2001) Persistent solar influence on North Atlantic climate during the Holocene. *Science*, 294(5549), 2130–2136.

Borchers, B., Marrero, S., Balco, G., Caffee, M., Goehring, B., Lifton, N. et al. (2016) Geological calibration of spallation production rates in the CRONUS-Earth project. *Quaternary Geochronology*, 31, 188–198.

Braucher, R., Guillou, V., Bourlès, D.L., Arnold, M., Aumaître, G., Keddadouche, K. et al. (2015) Preparation of ASTER in-house 10Be/9Be standard solutions. *Nuclear Instruments and Methods in Physics Research Section B: Beam Interactions with Materials and Atoms*, 361, 335–340.

Briner, J.P., Miller, G.H., Davis, P.T. & Finkel, R.C. (2005) Cosmogenic exposure dating in arctic glacial landscapes: implications for the glacial history of northeastern Baffin Island, Arctic Canada. *Canadian Journal of Earth Sciences*, 42(1), 67–84.

Briner, J.P., Overeem, I., Miller, G. & Finkel, R. (2007) The deglaciation of Clyde Inlet, northeastern Baffin Island, Arctic Canada. *Journal of Quaternary Science*, 22(3), 223–232.

Briner, J.P., Bini, A.C. & Anderson, R.S. (2009) Rapid early Holocene retreat of a Laurentide outlet glacier through an Arctic fjord. *Nature Geoscience*, 2(7), 496–499.

Briner, J.P., Cuzzone, J.K., Badgeley, J.A., Young, N.E., Steig, E.J., Morlighem, M. et al. (2020) Rate of mass loss from the Greenland Ice Sheet will exceed Holocene values this century. *Nature*, 586(7827), 70–74.

Bromley, G.R.M., Hall, B.L., Thompson, W.B., Kaplan, M.R., Garcia, J.L. & Schaefer, J.M. (2015) Late glacial fluctuations of the Laurentide ice sheet in the White Mountains of Maine and New Hampshire, USA. *Quaternary Research*, 83(3), 522–530.

Brouard, E. & Lajeunesse, P. (2019) Glacial to postglacial submarine landform assemblages in fiords of northeastern Baffin Island. *Geomorphology*, 330, 40–56.

Brouard, E., Roy, M., Godbout, P.M. & Veillette, J.J. (2021) A framework for the timing of the final meltwater outbursts from glacial Lake Agassiz-Ojibway. *Quaternary Science Reviews*, 274, 107269.

Bryson, R.A., Wendland, W.M., Ives, J.D. & Andrews, J.T. (1969) Radiocarbon isochrones on the disintegration of the Laurentide Ice Sheet. *Arctic and Alpine Research*, 1(1), 1–13.

Buizert, C., Gkinis, V., Severinghaus, J.P., He, F., Lecavalier, B.S., Kindler, P. et al. (2014) Greenland temperature response to climate forcing during the last deglaciation. *Science*, 345(6201), 1177–1180.

Carlson, A.E., LeGrande, A.N., Oppo, D.W., Came, R.E., Schmidt, G.A., Anslow, F.S. et al. (2008) Rapid early Holocene deglaciation of the Laurentide ice sheet. *Nature Geoscience*, 1(9), 620–624.

Carlson, A.E., Clark, P.U., Haley, B.A. & Klinkhammer, G.P. (2009) Routing of western Canadian Plains runoff during the 8.2 ka cold event. *Geophysical Research Letters*, 36, L14704.

Carlson, A.E. & Clark, P.U. (2012) Ice sheet sources of sea level rise and freshwater discharge during the last deglaciation. *Reviews of Geophysics*, 50(4), RG4007.

Carlson, A.E. (2020) Comment on: Deglaciation of the Greenland and Laurentide ice sheets interrupted by glacier advance during abrupt coolings. *Quaternary Science Reviews*, 240, 106354.

Chmeleff, J., von Blanckenburg, F., Kossert, K. & Jakob, D. (2010) Determination of the 10Be half-life by multicollector ICP-MS and liquid scintillation counting. *Nuclear Instruments and Methods in*

Physics Research Section B: Beam Interactions with Materials and Atoms, 268(2), 192–199.
Clark, C.D., Knight, J.K. & T. Gray, J. (2000) Geomorphological reconstruction of the Labrador sector of the Laurentide Ice Sheet. *Quaternary Science Reviews*, 19(13), 1343–1366.
Clark, P.U., Brook, E.J., Raisbeck, G.M., Yiou, F. & Clark, J. (2003) Cosmogenic 10Be ages of the Saglek Moraines, Torngat Mountains, Labrador. *Geology*, 31(7), 617–620.
Clarke, G.K.C., Leverington, D.W., Teller, J.T. & Dyke, A.S. (2004) Paleohydraulics of the last outburst flood from glacial Lake Agassiz and the 8200BP cold event. *Quaternary Science Reviews*, 23(3–4), 389–407.
Coleman, A.P. (1921) Northwestern part of Labrador and New Quebec. *Canada, Geological Survey*, Memoir 124, 68 p.
Crump, S.E., Young, N.E., Miller, G.H., Pendleton, S.L., Tulenko, J.P., Anderson, R.S. et al. (2020) Glacier expansion on Baffin Island during early Holocene cold reversals. *Quaternary Science Reviews*, 241, 106419.
Dalton, A.S., Margold, M., Stokes, C.R., Tarasov, L., Dyke, A.S., Adams, R.S. et al. (2020) An updated radiocarbon-based ice margin chronology for the last deglaciation of the North American Ice Sheet Complex. *Quaternary Science Reviews*, 234, 106223.
Davis, P.T., Bierman, P.R., Corbett, L.B. & Finkel, R.C. (2015) Cosmogenic exposure age evidence for rapid Laurentide deglaciation of the Katahdin area, west-central Maine, USA, 16 to 15 ka. *Quaternary Science Reviews*, 116, 95–105.
Denton, G.H. & Karlén, W. (1973) Holocene climatic variations—their pattern and possible cause. *Quaternary Research*, 3(2), 155–205.
Denton, G.H., Anderson, R.F., Toggweiler, J.R., Edwards, R.L., Schaefer, J.M. & Putnam, A.E. (2010) The last glacial termination. *Science*, 328(5986), 1652–1656.
Dietrich, P., Ghienne, J.F., Lajeunesse, P., Normandeau, A., Deschamps, R. & Razin, P. (2019) Deglacial sequences and glacio-isostatic adjustment: Quaternary compared with Ordovician glaciations. *Geological Society, London, Special Publications*, 475(1), 149–179.
Dubé-Loubert, H., Roy, M., Schaefer, J.M. & Clark, P.U. (2018) 10Be dating of former glacial Lake Naskaupi (Québec-Labrador) and timing of its discharges during the last deglaciation. *Quaternary Science Reviews*, 191, 31–40.
Dubois, J.M. & Dionne, J.C. (1985) The Québec North Shore moraine system: A major feature of Late Wisconsin déglaciation. *Geological Society of America Special*, Papers 197, 125–134.
Dyke, A.S. (1979) Glacial and sea-level history of southwestern Cumberland Peninsula, Baffin Island, NWT, Canada. *Arctic and Alpine Research*, 11(2), 179–202.
Dyke, A.S. & Prest, V.K. (1987) Late Wisconsinan and Holocene History of the Laurentide Ice Sheet. *Géographie physique et Quaternaire*, 41, 237–263.
Dyke, A.S., Moore, A. & Robertson, L. (2003) Deglaciation of North America: Thirty-two digital maps at 1:7 000 000 scale with accompanying digital chronological database and one poster (two sheets) with full map series. *Geological Survey Canada*, Open File 1574.
Engstrom, D.R. & Hansen, B.C.S. (1985) Postglacial vegetational change and soil development in southeastern Labrador as inferred from pollen and chemical stratigraphy. *Canadian Journal of Botany*, 63(3), 543–561.
Fitzhugh, W. (1973) Environmental approaches to the prehistory of the north. *Journal of the Washington Academy of Sciences*, 63, 39–53.
Fisher, T.G., Smith, D.G. & Andrews, J.T. (2002) Preboreal oscillation caused by a glacial Lake Agassiz flood. *Quaternary Science Reviews*, 21(8–9), 873–878.
Fleitmann, D., Mudelsee, M., Burns, S.J., Bradley, R.S., Kramers, J. & Matter, A. (2008) Evidence for a widespread climatic anomaly at around 9.2 ka before present. *Paleoceanography*, 23(1), n/a.
Fulton, R.J. & Hodgson, D.A. (1979). Wisconsin glacial retreat, Southern Labrador. Current Research, Part C, Geological Survey of Canada, Paper 79–1C, 17–21.
Gebhardt, C., Ohlendorf, C., Gross, F., Matthiessen, J. & Schneider, R. (2020) Development of the Labrador Shelf During the Past Glaciations, Cruise No. MSM84, June 19 to July 16, 2019, St. Johns (Canada) - St. Johns (Canada). Maria S. Merian Berichte, Gutachterpanel Forschungsschiffe, Bonn, 78 pp.
Grant, D.R. (1992) *Quaternary Geology of St. Anthony-Blanc-Sablon Area, Newfoundland and Quebec*. Geological Survey of Canada. 69 pp.
Greene, B.A. (1974) An outline of the geology of Labrador. *Geoscience Canada*, 1(3), 36–40.
Hardy, L. (1982) La moraine frontale de Sakami, Québec subarctique. *Géographie physique et Quaternaire*, 36(1–2), 51–61.
Harington, C.R., Anderson, T.W. & Rodrigues, C.G. (1993) Pleistocene walrus (Odobenus rosmarus) from Forteau, Labrador. *Géographie physique et Quaternaire*, 47(1), 111–118.
He, F. & Clark, P.U. (2022) Freshwater forcing of the atlantic meridional overturning circulation revisited. *Nature Climate Change*, 12(5), 449–454.
Heaton, T.J., Köhler, P., Butzin, M., Bard, E., Reimer, R.W., Austin, W.E.N., Bronk Ramsey, C., Grootes, P.M., Hughen, K.A., Kromer, B., Reimer, P.J., Adkins, J., Burke, A., Cook, M.S., Olsen, J. & Skinner, L.C. (2020) Marine20—The Marine Radiocarbon Age Calibration Curve (0–55,000 cal BP). *Radiocarbon*, 62(4), 779–820.
Hillaire-Marcel, C., Occhietti, S. & Vincent, J.S. (1981) Sakami moraine, Quebec: a 500-km-long moraine without climatic control. *Geology*, 9(5), 210–214.
Hodgson, D.A. & Fulton, R.J. (1972) Site description, age and significance of a shell sample from the mouth of the Michael River, 30 km south of Cape Harrison, Labrador. Report of Activities, Part B, Geological Survey of Canada, Paper 72–1, 102–105.
Hynes, A. & Rivers, T. (2010) Protracted continental collision—Evidence from the Grenville orogen. *Canadian Journal of Earth Sciences*, 47(5), 591–620.
Ives, J.D. (1978) The maximum extent of the Laurentide Ice Sheet along the east coast of North America during the last glaciation. *Arctic*, 31, 24–53.
Jamieson, S.S.R., Vieli, A., Livingstone, S.J., Cofaigh, C.Ó., Stokes, C., Hillenbrand, C.D. et al. (2012) Ice-stream stability on a reverse bed slope. *Nature Geoscience*, 5(11), 799–802.
Jansson, K.N. (2003) Early Holocene glacial lakes and ice marginal retreat pattern in Labrador/Ungava, Canada. *Palaeogeography, Palaeoclimatology, Palaeoecology*, 193(3–4), 473–501.
Jennings, A., Andrews, J., Pearce, C., Wilson, L. & Ólfasdótttir, S. (2015) Detrital carbonate peaks on the Labrador shelf, a 13–7 ka template for freshwater forcing from the Hudson Strait outlet of the Laurentide Ice Sheet into the subpolar gyre. *Quaternary Science Reviews*, 107, 62–80.
Jones, R.S., Small, D., Cahill, N., Bentley, M.J. & Whitehouse, P.L. (2019) iceTEA: Tools for plotting and analysing cosmogenic-nuclide surface-exposure data from former ice margins. *Quaternary Geochronology*, 51, 72–86.
Jordan, R. (1975) Pollen diagrams from Hamilton Inlet, central Labrador, and their environmental implications for the northern Maritime Archaic. *Arctic Anthropology*, 12(2), 92–116.
Josenhans, H.W., Zevenhuizen, J. & Klassen, R.A. (1986) The Quaternary geology of the Labrador Shelf. *Canadian Journal of Earth Sciences*, 23, 1190–1213.
King, G.A. (1985) A standard method for evaluating radiocarbon dates of local deglaciation: application to the deglaciation history of southern Labrador and adjacent Québec. *Géographie physique et Quaternaire*, 39(2), 163–182.
Klassen, R.A., Paradis, S., Bolduc, A.M. & Thomas, R.D. (1992) Glacial landforms and deposits, Labrador, Newfoundland and eastern Québec. Geological Survey of Canada, Map 1814A, scale 1:1 000 000.
Kleiven, H.F., Kissel, C., Laj, C., Ninnemann, U.S., Richter, T.O. & Cortijo, E. (2008) Reduced North Atlantic deep water coeval with the glacial Lake Agassiz freshwater outburst. *Science*, 319 (5859), 60–64.
Kobashi, T., Menviel, L., Jeltsch-Thömmes, A., Vinther, B.M., Box, J.E., Muscheler, R. et al. (2017) Volcanic influence on centennial to millennial Holocene Greenland temperature change. *Scientific reports*, 7(1), 1441.
Kohl, C.P. & Nishiizumi, K. (1992) Chemical isolation of quartz for measurement of in-situ-produced cosmogenic nuclides. *Geochimica et Cosmochimica Acta*, 56, 3583–3587.
Korschinek, G., Bergmaier, A., Faestermann, T., Gerstmann, U.C., Knie, K., Rugel, G. et al. (2010) A new value for the half-life of 10Be by heavy-ion elastic recoil detection and liquid scintillation counting.

Nuclear Instruments and Methods in Physics Research Section B: Beam Interactions with Materials and Atoms, 268(2), 187–191.
Lajeunesse, P. & Allard, M. (2003) The Nastapoka drift belt, eastern Hudson Bay: implications of a stillstand of the Quebec Labrador ice margin in the Tyrrell Sea at 8 ka BP. *Canadian Journal of Earth Sciences*, 40(1), 65–76.
Lajeunesse, P. & St-Onge, G. (2008) The subglacial origin of the Lake Agassiz–Ojibway final outburst flood. *Nature Geoscience*, 1(3), 184–188.
Lajeunesse, P., Dietrich, P. & Ghienne, J.F. (2019) Late Wisconsinan grounding zones of the Laurentide Ice Sheet margin off the Québec North Shore (NW Gulf of St Lawrence). *Geological Society, London, Special Publications*, 475(1), 241–259.
Lal, D. (1991) Cosmic ray labeling of erosion surfaces: in situ nuclide production rates and erosion models. *Earth and Planetary Science Letters*, 104, 424–439.
Lamb, H.F. (1978) Post-glacial Vegetation Change in Southeastern Labrador, M. Sc. thesis. University of Minnesota, Minneapolis, Minnesota, 101 p.
Lamb, H.F. (1980) Late Quaternary vegetational history of southeastern Labrador. *Arctic and Alpine Research*, 12(2), 117–135.
Lamb, H.F. (1985) Palynological evidence for postglacial change in the position of tree limit in Labrador. *Ecological Monographs*, 55(2), 241–258.
Lesnek, A.J. & Briner, J.P. (2018) Response of a land-terminating sector of the western Greenland Ice Sheet to early Holocene climate change: evidence from ^{10}Be dating in the Søndre Isortoq region. *Quaternary Science Reviews*, 180, 145–156.
Leydet, D.J., Carlson, A.E., Teller, J.T., Breckenridge, A., Barth, A.M., Ullman, D.J. et al. (2018) Opening of glacial Lake Agassiz's eastern outlets by the start of the Younger Dryas cold period. *Geology*, 46(2), 155–158.
Lifton, N., Sato, T. & Dunai, T.J. (2014) Scaling in situ cosmogenic nuclide production rates using analytical approximations to atmospheric cosmic-ray fluxes. *Earth and Planetary Science Letters*, 386, 149–160.
Long, A.J., Woodroffe, S.A., Dawson, S., Roberts, D.H. & Bryant, C.L. (2009) Late Holocene relative sea level rise and the Neoglacial history of the Greenland ice sheet. *Journal of Quaternary Science*, 24(4), 345–359.
Lowdon, J.A. & Blake Jr., W. (1973) Geological Survey of Canada radiocarbon dates XIII, Geological Survey of Canada, Paper 73–7, 61 p.
Lowdon, J.A. & Blake Jr., W. (1975) Geological Survey of Canada radiocarbon dates XV, Geological Survey of Canada, Paper 75–7, 32 p.
Lowdon, J.A. & Blake Jr., W. (1979) Geological Survey of Canada radiocarbon dates XIX; Geological Survey of Canada, Paper 79–7, 58 p.
Lowdon, J.A. & Blake Jr., W. (1980) Geological Survey of Canada radiocarbon dates XX, Geological Survey of Canada, Paper 80–7, 28 p.
Lowell, T.V., Kelly, M.A., Howley, J.A., Fisher, T.G., Barnett, P.J., Schwart, R. et al. (2021) Near-constant retreat rate of a terrestrial margin of the Laurentide Ice Sheet during the last deglaciation. *Geology*, 49(12), 1511–1515.
Margreth, A., Gosse, J.C. & Dyke, A.S. (2017) Wisconsinan and early Holocene glacial dynamics of Cumberland peninsula, Baffin Island, arctic Canada. *Quaternary Science Reviews*, 168, 79–100.
Marsella, K.A., Bierman, P.R., Davis, P.T. & Caffee, M.W. (2000) Cosmogenic 10Be and 26Al ages for the last glacial maximum, eastern Baffin Island, Arctic Canada. *Geological Society of America Bulletin*, 112(8), 1296–1312.
McManus, J.F., Francois, R., Gherardi, J.M., Keigwin, L.D. & Brown-Leger, S. (2004) Collapse and rapid resumption of Atlantic meridional circulation linked to deglacial climate changes. *Nature*, 428(6985), 834–837.
McNeely, R., Dyke, A.S. & Southon, J.R. (2006) Canadian marine reservoir ages, preliminary data assessment. Geological Survey of Canada, Open File 5049.
Miller, G.H. (1980) Late foxe glaciation of southern Baffin Island, NWT, Canada. *Geological Society of America Bulletin*, 91(7), 399–405.
Morrill, C., Anderson, D.M., Bauer, B.A., Buckner, R., Gille, E.P., Gross, W.S. et al. (2013) Proxy benchmarks for intercomparison of 8.2 ka simulations. *Climate of the Past*, 9(1), 423–432.
Morrison, A. (1970) Pollen diagrams from interior Labrador. *Canadian Journal of Botany*, 48(11), 1957–1975.
Occhietti, S. (2007) The Saint-Narcisse morainic complex and early Younger Dryas events on the southeastern margin of the Laurentide Ice Sheet. *Géographie physique et Quaternaire*, 61(2–3), 89–117.
Occhietti, S., Parent, M., Lajeunesse, P., Robert, F. & Govare, E. (2011) Late Pleistocene–Early Holocene decay of the Laurentide Ice Sheet in Québec–Labrador. *Developments in Quaternary Science*, 15, 601–630.
Piper, D.J.W. (1991) Seabed geology of the Canadian eastern continental shelf. *Continental Shelf Research*, 11(8–10), 1013–1035.
Putnam, A.E., Bromley, G.R.M., Rademaker, K. & Schaefer, J.M. (2019) In situ 10Be production-rate calibration from a 14C-dated late-glacial moraine belt in Rannoch Moor, central Scottish Highlands. *Quaternary Geochronology*, 50, 109–125.
Rasmussen, S.O., Bigler, M., Blockley, S.P., Blunier, T., Buchardt, S.L., Clausen, H.B. et al. (2014) A stratigraphic framework for abrupt climatic changes during the Last Glacial period based on three synchronized Greenland ice-core records: refining and extending the INTIMATE event stratigraphy. *Quaternary Science Reviews*, 106, 14–28.
Recq, C., Bhiry, N., Todisco, D., Buisson, E., Lauer, T. & Rinterknecht, V.R. (2020) Local records of former ice-sheet margins: geomorphological dynamics and sea-level evolution in the Nain archipelago (Labrador, Atlantic Canada). In GSA 2020 Connects Online.
Reimer, P.J., Austin, W.E.N., Bard, E., Bayliss, A., Blackwell, P.G., Bronk Ramsey, C. et al. (2020) The IntCal20 northern Hemisphere radiocarbon age calibration curve (0-55 cal kBP), *Radiocarbon*, 62(4), 725–757.
Richard, P.J.H., Larouche, A. & Bouchard, M.A. (1982) Âge de la déglaciation finale et histoire postglaciaire de la végétation dans la partie centrale du Nouveau-Québec. *Géographie Physique et Quaternaire*, 36, 63–90.
Roger, J., Saint-Ange, F., Lajeunesse, P., Duchesne, M.J. & St-Onge, G. (2013) Late Quaternary glacial history and meltwater discharges along the Northeastern Newfoundland Shelf. *Canadian Journal of Earth Sciences*, 50(12), 1178–1194.
Rohling, E.J. & Pälike, H. (2005) Centennial-scale climate cooling with a sudden cold event around 8,200 years ago. *Nature*, 434(7036), 975–979.
Shakun, J.D., Clark, P.U., He, F., Marcott, S.A., Mix, A.C., Liu, Z., Otto-Bliesner, B., Schmittner, A., & Bard, E. (2012) Global warming preceded by increasing carbon dioxide concentrations during the last deglaciation. *Nature*, 484(7392), 49–54.
Shaw, J., Piper, D.J.W., Fader, G.B.J., King, E.L., Todd, B.J., Bell, T. et al. (2006) A conceptual model of the deglaciation of Atlantic Canada. *Quaternary Science Reviews*, 25(17–18), 2059–2081.
Stone, J.O. (2000) Air pressure and cosmogenic isotope production. *Journal of Geophysical Research*, 105(B10), 23753–23759.
Stuiver, M. & Reimer, P.J. (1993) Extended14C Data Base and Revised CALIB 3.014C Age Calibration Program. *Radiocarbon*, 35, 215–230.
Süfke, F., Gutjahr, M., Keigwin, L.D., Reilly, B., Giosan, L. & Lippold, J. (2022) Arctic drainage of Laurentide Ice Sheet meltwater throughout the past 14,700 years. *Communications Earth & Environment*, 3(1), 1–11.
Syvitski, J.P.M. & Lee, H.J. (1997) Postglacial sequence stratigraphy of Lake Melville, Labrador. *Marine Geology*, 143(1–4), 55–79.
Ullman, D.J. Carlson, A.E., Hostetler, S.W., Clark, P.U., Cuzzone, J., Milne, G.A. et al. (2016) Final Laurentide ice-sheet deglaciation and Holocene climate-sea level change. *Quaternary Science Reviews*, 152, 49–59.
Vilks, G. & Mudie, P.J. (1978) Early deglaciation of the Labrador Shelf. *Science*, 202(4373), 1181–1183.
Vilks, G., Hardy, I.A. & Josenhans, H.W. (1984) Late Quaternary stratigraphy of the inner Labrador Shelf. Current Research, part A. Geological Survey of Canada, Paper 84–1A, 57–65.
Vilks, G., Deonarine, B. & Winters, G. (1987) Late Quaternary marine geology of Lake Melville, Labrador. Geological Survey of Canada, Paper 87–22, 50 p.

von Grafenstein, U., Erlenkeuser, H., Müller, J., Jouzel, J. & Johnsen, S. (1998) The cold event 8200 years ago documented in oxygen isotope records of precipitation in Europe and Greenland. *Climate Dynamics*, 14(2), 73–81.

Young, N.E., Briner, J.P., Rood, D.H. & Finkel, R.C. (2012) Glacier extent during the Younger Dryas and 8.2-ka event on Baffin Island, Arctic Canada. *Science*, 337(6100), 1330–1333.

Young, N.E., Schaefer, J.M., Briner, J.P. & Goehring, B.M. (2013) A 10Be production-rate calibration for the Arctic. *Journal of Quaternary Science*, 28(5), 515–526.

Young, N.E., Briner, J.P., Miller, G.H., Lesnek, A.J., Crump, S.E., Thomas, E.K. et al. (2020a) Deglaciation of the Greenland and Laurentide ice sheets interrupted by glacier advance during abrupt coolings. *Quaternary Science Reviews*, 229, 106091.

Young, N.E., Briner, J.P., Schaefer, J.M., Miller, G.H., Lesnek, A.J., Crump, S.E. et al. (2020b) Reply to Carlson (2020) comment on "Deglaciation of the Greenland and Laurentide ice sheets interrupted by glacier advance during abrupt coolings". *Quaternary Science Reviews*, 240, 106354.

Young, N.E., Briner, J.P., Miller, G.H., Lesnek, A.J., Crump, S.E., Pendleton, S.L. et al. (2021) Pulsebeat of early Holocene glaciation in Baffin Bay from high-resolution beryllium-10 moraine chronologies. *Quaternary Science Reviews*, 270, 107179.

Yu, S.Y., Colman, S.M., Lowell, T.V., Milne, G.A., Fisher, T.G., Breckenridge, A. et al. (2010) Freshwater outburst from Lake Superior as a trigger for the cold event 9300 years ago. *Science*, 328(5983), 1262–1266.